

Physical Analysis of Spherical Stellar Structures in $f(Q, T)$ Theory

M. Zeeshan Gul ^{*}, M. Sharif [†] and Adeeba Arooj [‡]

Department of Mathematics and Statistics, The University of Lahore,
1-KM Defence Road Lahore-54000, Pakistan.

Abstract

This paper explores the viability and stability of compact stellar objects characterized by anisotropic matter in the framework of $f(Q, T)$ theory, where Q denotes non-metricity and T represents the trace of the energy-momentum tensor. We consider a specific model of this theory to obtain explicit expressions for the field equations governing the behavior of matter and geometry in this context. Furthermore, the Karmarkar condition is employed to assess the configuration of static spherically symmetric structures. The values of unknown constants in the metric potentials are determined through matching conditions of the interior and exterior spacetimes. Various physical quantities such as fluid parameters, energy constraints, equation of state parameters, mass, compactness and redshift are graphically analyzed to evaluate the viability of the considered compact stars. The Tolman-Oppenheimer-Volkoff equation is used to examine the equilibrium state of the stellar models. Moreover, the stability of the proposed compact stars is investigated through sound speed and adiabatic index methods. This study concludes that the proposed compact stars analyzed in this theoretical framework are viable and stable, as all the required conditions are satisfied.

Keywords: $f(Q, T)$ theory; Compact objects; Matching conditions.

PACS: 97.60.Jd; 04.50.Kd; 98.35.Ac; 97.10.-q.

^{*}mzeeshangul.math@gmail.com

[†]msharif.math@pu.edu.pk

[‡]aarooj933@gmail.com

1 Introduction

Stars serve as vital constituents of galaxies and maintain equilibrium by balancing the inward gravitational force with the outward pressure generated through nuclear fusion reactions. When a star depletes its nuclear fuel, it may no longer generate sufficient pressure to counteract gravitational collapse. This results in the creation of compact objects such as white dwarfs, neutron stars or black holes, depending on their initial mass. Neutron stars are the most captivating cosmic objects that play pivotal roles in various astrophysical processes. The intense magnetic fields surrounding neutron stars lead to the emission of intense radiation, particularly in the form of X-rays and gamma rays. Furthermore, neutron stars have significant influence in astrophysical phenomena, including the formation of heavy elements in the universe and the generation of gravitational waves.

Advances in observational techniques, such as the development of X-rays and radio telescopes have enabled scientists to make significant progress in the detection and study of neutron stars. These observations have not only opened up novel avenues for research but have also deepened our comprehension of the fundamental processes that govern the universe. Baade and Zwicky [1] argued that compact stars (CSs) are formed as a result of supernovae and their existence has been proved by the discovery of pulsars [2]. Pulsars have captured the attention of many researchers due to their extraordinary attributes such as extreme density, powerful magnetic fields and rapid rotation, which results in neutron stars emitting beams of electromagnetic radiation. These beams manifest as regular pulses of radiation, leading to the name “pulsar”. The exploration of neutron stars and pulsars provides researchers with insights into diverse aspects of these captivating objects, including their mass, radius, magnetic fields, rotational dynamics and behavior under extreme conditions. The viable behavior of pulsars with various consideration has been studied in [3]. Mak and Harko [4] discussed viable features of rotating neutron stars and their stability through the Herrera cracking approach.

Researchers have employed various approaches, including solving metric elements, imposing constraints on fluid parameters and utilizing specific equations of state to study the geometry of CSs. Among these methods, the Karmarkar method stands out as a valuable mathematical tool for exploring the interior geometry of CSs. This method has been widely applied by numerous researchers to gain insights into the physical characteristics and stability

of the cosmic objects. By establishing a correlation between temporal and radial elements, the Karmarkar method aids in comprehending the nature of the celestial objects. Specifically, the Karmarkar condition is formulated for analyzing solutions in the context of static spherical spacetime [5]. Maurya et al [6] delved into the physically viable characteristics of anisotropic CSs using this technique. Singh and Pant [7] used the Karmarkar condition to investigate the interior geometry of celestial objects. Bhar et al [8] employed this method to analyze the viability and stability of anisotropic CSs.

Einstein's general theory of relativity (EGTR) is a fundamental theory in physics that has revolutionized our comprehension of gravity and the nature of spacetime. Regarded as the cornerstone of modern physics, EGTR relies on Riemannian geometry which involves the mathematical notion of a metric space. In this framework, spacetime is characterized by geometric structures defined by Riemann's metric. Additionally, EGTR's expansion provides insights into the gravitational field and the behavior of matter on cosmic scales. In contrast, Weyl [9] developed a more comprehensive geometric framework by introducing the concept of the length connection, aiming to unify the fundamental forces of nature. This connection does not primarily concern with the length of vectors during parallel transport but rather focuses on adjusting or gauging the conformal factor. Weyl's theory introduces the notion of non-metricity by positing that the covariant divergence of the metric tensor is non-zero.

Non-Riemannian geometries serve as extensions to Riemannian geometry, offering broader descriptions of spacetime curvature through the inclusion of torsion and non-metricity concepts. The non-metricity scalar is a mathematical quantity which provides an alternative explanation for cosmic expansion beyond the standard cosmological model, which relies on dark energy [10]. Teleparallel gravity is introduced as an alternative theory to EGTR, where torsion (\mathcal{T}) represents gravitational interaction. Unlike the Levi-Civita connection in EGTR, the teleparallel equivalent to EGTR exhibits both non-metricity and zero curvature. The integral actions for torsion curvature and non-metricity are formulated as $\int \sqrt{-g}\mathcal{T}$ [11] and $\int \sqrt{-g}Q$ [12], respectively. Researchers have developed a range of extended gravitational theories to address these challenges and delve deeper into the mysteries of the cosmos [13]-[26].

The modified symmetric teleparallel theory is further extended by incorporating the trace of stress-energy tensor in the functional action, named as $f(Q, T)$ theory [27]. This extension establishes a specific coupling between

the trace of the energy-momentum tensor and non-metricity, attracting significant attention of researchers for its profound implications in the realm of gravitational physics. The modifications introduced by $f(Q, T)$ gravity have an impact on the internal structure of CSs. This influences changes in the relationship between pressure and density, variations in stellar radii and mass profiles. The corresponding equations of motion play a role in hydrostatic equilibrium and affect the stability of the star. Deviations from the predictions of EGTR may rise to unique mass-radius relations that can be tested against observational data from X-ray binaries. Neutron stars are prime sources of gravitational waves in binary systems. The modifications introduced by $f(Q, T)$ gravity can lead to distinct gravitational wave signatures that may differ from those predicted by EGTR. Furthermore, the implications of $f(Q, T)$ gravity may extend to other properties like surface redshift, providing avenues for distinguishing this gravity model from other theories in the context of CSs.

The presence of additional correction terms in this modified framework has been underscored by noteworthy outcomes, potentially exerting a substantial influence on the geometric viability in comparison to EGTR. The $f(Q, T)$ theory is employed as a mathematical tool to scrutinize obscure aspects of gravitational dynamics on a large scale. Investigations into this modified theory have extended to its implications for cosmic models and the accelerated expansion of the universe. The motivation driving the exploration of this theory encompasses an examination of its theoretical implications, its alignment with observational data and its significance in cosmological contexts. Arora et al [28] assured that $f(Q, T)$ gravity discusses late-time acceleration of the cosmos. Bhattacharjee et al [29] scrutinized the phenomenon of baryogenesis in the $f(Q, T)$ theory. Arora and Sahoo [30] studied the transitions between accelerated and decelerated phases of the universe expansion through deceleration parameter, indicating that the dynamics of cosmic expansion can be accounted for $f(Q, T)$ theory. Xu et al [31] predicted a de Sitter type cosmic expansion in this framework proposing it as an alternative explanation of dark energy. Najera and Fajardo [32] assured that this gravity offers alternation to the standard cosmological model (Λ CDM) suggesting deviations from conventional frameworks. Godani and Samanta [33] studied the cosmic evolution using various cosmic parameters in this theory, as it accounts for the accelerated cosmic expansion. Agrawal et al [34] demonstrated the existence of matter bounce scenario in $f(Q, T)$ gravity, which offers alternative cosmological scenario to the Big Bang. Pradhan et al [35] studied

physical properties to ensure the existence of a stable gravastar model within the modified theory that suggest alternative configurations for CSs.

The intriguing properties of CSs yield captivating results in the context of alternative gravitational theories. Arapoglu et al [36] employed perturbation techniques to investigate the geometry of CSs in $f(R)$ gravity. They explored how deviations from the EGTR impact the structure of compact objects. In the same theoretical framework, Astashenok et al [37] delved into the structural aspects of pulsars with anisotropic matter configurations. Das et al [38] explored the influence of effective matter variables on the geometry of anisotropic spheres in $f(R, T)$ theory. Deb et al [39] analyzed the geometry of spherically symmetric strange stars in a similar context. Biswas et al [40] discussed strange quark stars using the Krori-Barua solution in the context of curvature-matter coupled theory. Bhar et al [41] explored the viable characteristics of a 4U 1538-52 CS in Einstein Gauss-Bonnet gravity. In $f(G)$ theory, Sharif and Ramzan [42] studied the behavior of various physical quantities and the stability of distinct CSs. Dey et al [43] employed the Finch-Skea symmetry to examine the viability of anisotropic stellar models in $f(R, T)$ theory. Sharif and his collaborators studied the Noether symmetry approach [44]-[50], stability of the Einstein universe [51]-[53] and dynamics of gravitational collapse [54]-[58] and static spherically symmetric structures [59]-[61] in $f(R, T^2)$ theory. Recently, the study of observational constraints in modified gravities discussed in [62]-[63].

The above literature motivates us to investigate the viable characteristics of anisotropic CSs in the context of $f(Q, T)$ theory. We use the following format in the paper. Section 2 presents the fundamental formulation of $f(Q, T)$ gravity. In section 3, a specific model of this theory is considered to derive explicit expressions for energy density and pressure components. We evaluate unknown parameters through the matching conditions. In Section 4, various physical quantities are used to determine the physical features of the considered CSs. Furthermore, the equilibrium state and the stability of the considered CSs are analyzed in Section 5. We compile our findings in Section 6

2 $f(Q, T)$ Theory: Basic Formalism

This section introduces the fundamental framework of the modified $f(Q, T)$ theory and outlines the derivation of field equations through the variational

principle. Weyl [9] extended Riemannian geometry to serve as a mathematical foundation for describing gravitation in the framework of EGTR. In Riemannian geometry, the direction and length of a vector remain unchanged during parallel transport around a closed path. However, Weyl proposed a modification where a vector undergoes both directional and length changes during such transport. This modification introduces a new vector field (h^μ) that characterizes the geometric aspects of Weyl geometry. The key fields in Weyl's space include this new vector field and the metric tensor. While the metric tensor defines the local structure of spacetime, specifying distances and angles, the vector field is introduced to account for length changes during parallel transport. Weyl's theory posits that the vector field shares mathematical properties with electromagnetic potentials in physics, suggesting a profound connection between gravitational and electromagnetic forces. Weyl's proposal implies a common geometric origin for these forces [64].

In Weyl geometry, transporting a vector along an infinitesimal path results in a change in its length as $\delta l = l h_\mu \delta x^\mu$ [64]. This signifies that the variation in the vector's length is directly proportional to the original length, the connection coefficient, and the displacement along the path. When the vector is transported in parallel around a small closed loop in Weyl space, the variation in its length can be described as follows

$$\delta l = l \Psi_{\mu\nu} \delta s^{\mu\nu}, \quad \Psi_{\mu\nu} = \nabla_\nu h_\mu - \nabla_\mu h_\nu. \quad (1)$$

This states that the variation in the vector's length is proportional to the original length (l), the curvature of the Weyl connection (Ψ) and the area enclosed by the loop ($\delta s^{\mu\nu}$). A local scaling length of the form $\bar{l} = \phi(x)l$ changes the field h_μ to $\bar{h}_\mu = h_\mu + (\ln \phi)_{,\mu}$, whereas the elements of metric tensor are modified by the conformal transformations $\bar{g}_{\mu\nu} = \phi^2 g_{\mu\nu}$ and $\bar{g}^{\mu\nu} = \phi^{-2} g^{\mu\nu}$, respectively [65]. A semi-metric connection is another important feature of the Weyl geometry, defined as

$$\bar{\Gamma}_{\mu\nu}^\lambda = \Gamma_{\mu\nu}^\lambda + g_{\mu\nu} h^\lambda - \delta_\mu^\lambda h_\nu - \delta_\nu^\lambda h_\mu, \quad (2)$$

where $\Gamma_{\mu\nu}^\lambda$ denotes the Christoffel symbol. One can construct a gauge covariant derivative based on the supposition that $\bar{\Gamma}_{\mu\nu}^\lambda$ is symmetric [65]. The Weyl curvature tensor using the covariant derivative can be expressed as

$$\bar{C}_{\mu\nu\lambda\xi} = \bar{C}_{(\mu\nu)\lambda\xi} + \bar{C}_{[\mu\nu]\lambda\xi}, \quad (3)$$

where

$$\begin{aligned}
\bar{\mathcal{C}}_{[\mu\nu]\lambda\xi} &= \mathcal{C}_{\mu\nu\lambda\xi} + 2\nabla_\lambda h_{[\mu g_\nu]\xi} + 2\nabla_\xi h_{[\nu g_\mu]\lambda} + 2h_\lambda h_{[\mu g_\nu]\xi} + 2h_\xi h_{[\nu g_\mu]\lambda} \\
&\quad - 2h^2 g_{\lambda[\mu g_\nu]\xi}, \\
\bar{\mathcal{C}}_{(\mu\nu)\lambda\xi} &= \frac{1}{2}(\bar{\mathcal{C}}_{\mu\nu\lambda\xi} + \bar{\mathcal{C}}_{\nu\mu\lambda\xi}), \\
&= g_{\mu\nu} \Psi_{\lambda\xi}.
\end{aligned}$$

The Weyl curvature tensor after the first contraction yields

$$\bar{\mathcal{C}}_\nu^\mu = \bar{\mathcal{C}}_{\lambda\nu}^{\lambda\mu} = \mathcal{C}_\nu^\mu + 2h^\mu h_\nu + 3\nabla_\nu h^\mu - \nabla_\mu h^\nu + g_\nu^\mu (\nabla_\lambda h^\lambda - 2h_\lambda h^\lambda). \quad (4)$$

Finally, we obtain Weyl scalar as

$$\bar{\mathcal{C}} = \bar{\mathcal{C}}_\lambda^\lambda = \mathcal{C} + 6(\nabla_\mu h^\mu - h_\mu h^\mu). \quad (5)$$

Weyl-Cartan (WC) spaces incorporates torsion which provides a more expansive framework compared to Riemannian and Weyl geometry. This extended geometric structure serves as a versatile model for gravity theories, accommodating diverse scales and behaviors in parallel transport. Such investigations are particularly relevant for exploring alternative gravity theories or pursuing the unification of gravity with other fundamental forces. In a WC spacetime, vector length is defined by a symmetric metric tensor, and the rule for parallel transport is dictated by an asymmetric connection expressed as $d\varpi^\mu = -\varpi^\lambda \Gamma_{\lambda\nu}^\mu dx^\nu$ [66]. The connection for the WC geometry is expressed as

$$\tilde{\Gamma}_{\mu\nu}^\lambda = \Gamma_{\mu\nu}^\lambda + \mathcal{W}_{\mu\nu}^\lambda + L_{\mu\nu}^\lambda, \quad (6)$$

where $\mathcal{W}_{\mu\nu}^\lambda$ is the contorsion tensor and $L_{\mu\nu}^\lambda$ is the deformation tensor. The contorsion tensor from the torsion tensor can be obtained as

$$\mathcal{W}_{\mu\nu}^\lambda = \tilde{\Gamma}_{[\mu\nu]}^\lambda + g^{\lambda\xi} g_{\mu\varsigma} \tilde{\Gamma}_{[\nu\xi]}^\varsigma + g^{\lambda\xi} g_{\nu\varsigma} \tilde{\Gamma}_{[\mu\xi]}^\varsigma. \quad (7)$$

The non-metricity yields the deformation tensor as

$$L_{\mu\nu}^\lambda = \frac{1}{2} g^{\lambda\xi} (Q_{\nu\mu\xi} + Q_{\mu\nu\xi} - Q_{\lambda\mu\nu}), \quad (8)$$

where

$$Q_{\lambda\mu\nu} = \nabla_\lambda g_{\mu\nu} = -\partial g_{\mu\nu,\lambda} + g_{\nu\xi} \tilde{\Gamma}_{\mu\lambda}^\xi + g_{\xi\mu} \tilde{\Gamma}_{\nu\lambda}^\xi, \quad (9)$$

and $\tilde{\Gamma}_{\mu\nu}^\lambda$ is WC connection. Equations (2) and (6) indicate that the WC geometry with zero torsion is a particular case of Weyl geometry, where the non-metricity is defined as $Q_{\lambda\mu\nu} = -2g_{\mu\nu}h_\lambda$. Therefore, Eq.(6) turns out to be

$$\tilde{\Gamma}_{\mu\nu}^\lambda = \Gamma_{\mu\nu}^\lambda + g_{\mu\nu}h^\lambda - \delta_\mu^\lambda h_\nu - \delta_\nu^\lambda h_\mu + \mathcal{W}_{\mu\nu}^\lambda, \quad (10)$$

where

$$\mathcal{W}_{\mu\nu}^\lambda = \mathcal{T}_{\mu\nu}^\lambda - g^{\lambda\xi}g_{\xi\mu}\mathcal{T}_{\xi\nu}^\zeta - g^{\lambda\xi}g_{\xi\nu}\mathcal{T}_{\xi\mu}^\zeta, \quad (11)$$

is the contortion and the WC torsion is expressed as

$$\mathcal{T}_{\mu\nu}^\lambda = \frac{1}{2}(\tilde{\Gamma}_{\mu\nu}^\lambda - \tilde{\Gamma}_{\nu\mu}^\lambda). \quad (12)$$

The WC curvature tensor with the use of the connection is defined as

$$\tilde{\mathcal{C}}_{\mu\nu\xi}^\lambda = \tilde{\Gamma}_{\mu\xi,\nu}^\lambda - \tilde{\Gamma}_{\mu\nu,\xi}^\lambda + \tilde{\Gamma}_{\mu\xi}^\lambda\tilde{\Gamma}_{\lambda\nu}^\zeta - \tilde{\Gamma}_{\mu\nu}^\lambda\tilde{\Gamma}_{\lambda\xi}^\zeta. \quad (13)$$

The WC scalar can be obtained by contracting the curvature tensor as

$$\begin{aligned} \tilde{\mathcal{C}} &= \tilde{\mathcal{C}}_{\mu\nu}^{\mu\nu} = \mathcal{C} + 6\nabla_\nu h^\nu - 4\nabla_\nu \mathcal{T}^\nu - 6h_\nu h^\nu + 8h_\nu \mathcal{T}^\nu + \mathcal{T}^{\mu\lambda\nu}\mathcal{T}_{\mu\lambda\nu} \\ &+ 2\mathcal{T}^{\mu\lambda\nu}\mathcal{T}_{\nu\lambda\mu} - 4\mathcal{T}^\nu\mathcal{T}_\nu, \end{aligned} \quad (14)$$

where $\mathcal{T}_\nu = \mathcal{T}_{\mu\nu}^\mu$ and all covariant derivatives are considered corresponding to the metric.

The gravitational action can be reformulated by eliminating the boundary terms in the Ricci scalar as [67]

$$\mathcal{I} = \frac{1}{2\kappa} \int g^{\mu\nu} (\Gamma_{\xi\mu}^\lambda \Gamma_{\lambda\nu}^\xi - \Gamma_{\xi\lambda}^\lambda \Gamma_{\mu\nu}^\xi) \sqrt{-g} d^4x. \quad (15)$$

Based on the assumption that the connection is symmetric, we have

$$\Gamma_{\mu\nu}^\lambda = -L_{\mu\nu}^\lambda. \quad (16)$$

Thus the gravitational action becomes

$$\mathcal{I} = \frac{1}{2\kappa} \int -g^{\mu\nu} (L_{\xi\mu}^\lambda L_{\lambda\nu}^\xi - L_{\xi\lambda}^\lambda L_{\mu\nu}^\xi) \sqrt{-g} d^4x, \quad (17)$$

where

$$Q \equiv -g^{\mu\nu} (L_{\xi\mu}^\lambda L_{\lambda\nu}^\xi - L_{\xi\lambda}^\lambda L_{\mu\nu}^\xi), \quad (18)$$

with

$$L_{\xi\mu}^{\lambda} \equiv -\frac{1}{2}g^{\lambda\varsigma}(\nabla_{\mu}g_{\xi\varsigma} + \nabla_{\xi}g_{\varsigma\lambda} - \nabla_{\varsigma}g_{\xi\mu}). \quad (19)$$

From Eq.(17), one can obtain the gravitational action of $f(Q)$ theory by replacing non-mitricity scalar with an arbitrary function as

$$\mathcal{I} = \frac{1}{2\kappa} \int \sqrt{-g}f(Q)d^4x. \quad (20)$$

This is the action of symmetric teleparallel theory, which is a theoretical framework that provides an alternative geometric description of gravity.

Now, we extend this gravitational Lagrangian by introducing the trace of energy-momentum tensor in the functional action as

$$\mathcal{I} = \frac{1}{2\kappa} \int f(Q, T)\sqrt{-g}d^4x. \quad (21)$$

The modified Einstein-Hilbert action of $f(Q, T)$ gravity is defined as [27]

$$\mathcal{I} = \frac{1}{2\kappa} \int f(Q, T)\sqrt{-g}d^4x + \int L_m\sqrt{-g}d^4x. \quad (22)$$

The non-mitricity scalar is defined as

$$Q_{\lambda} \equiv Q_{\lambda}^{\mu}{}_{\mu}, \quad \tilde{Q}_{\lambda} \equiv Q_{\lambda\mu}^{\mu}. \quad (23)$$

The superpotential of this model is given by

$$P_{\mu\nu}^{\lambda} = -\frac{1}{2}L_{\mu\nu}^{\lambda} + \frac{1}{4}(Q^{\lambda} - \tilde{Q}^{\lambda})g_{\mu\nu} - \frac{1}{4}\delta_{(\mu}^{\lambda}Q_{\nu)}, \quad (24)$$

and the relation for Q is

$$Q = -Q_{\lambda\mu\nu}P^{\lambda\mu\nu} = -\frac{1}{4}(-Q^{\lambda\nu\xi}Q_{\lambda\nu\xi} + 2Q^{\lambda\nu\xi}Q_{\xi\lambda\nu} - 2Q^{\xi}\tilde{Q}_{\xi} + Q^{\xi}Q_{\xi}). \quad (25)$$

The calculation of the above relation is shown in Appendix **A**. By varying Eq.(22) with respect to the metric tensor, we obtain

$$\begin{aligned} \delta\mathcal{I} &= \int \frac{1}{2\kappa}\delta[f(Q, T)\sqrt{-g}] + \delta[L_m\sqrt{-g}]d^4x, \\ &= \int \frac{1}{2\kappa}\left[-\frac{1}{2}fg_{\mu\nu}\sqrt{-g}\delta g^{\mu\nu} + f_Q\sqrt{-g}\delta Q + f_T\sqrt{-g}\delta T\right] \end{aligned}$$

$$- \frac{1}{2} T_{\mu\nu} \sqrt{-g} \delta g^{\mu\nu} d^4 x. \quad (26)$$

The explicit formulation of δQ is given in Appendix B. Moreover, we define

$$T_{\mu\nu} \equiv \frac{-2}{\sqrt{-g}} \frac{\delta(\sqrt{-g} L_m)}{\delta g^{\mu\nu}}, \quad \Theta_{\mu\nu} \equiv g^{\lambda\xi} \frac{\delta T_{\lambda\xi}}{\delta g^{\mu\nu}}, \quad (27)$$

which implies that $\delta T = \delta(T_{\mu\nu} g^{\mu\nu}) = (T_{\mu\nu} + \Theta_{\mu\nu}) \delta g^{\mu\nu}$. Thus, Eq.(26) turns out to be

$$\begin{aligned} \delta \mathcal{I} = & \int \frac{1}{2\kappa} \left[\frac{-1}{2} f g_{\mu\nu} \sqrt{-g} \delta g^{\mu\nu} + f_T (T_{\mu\nu} + \Theta_{\mu\nu}) \sqrt{-g} \delta g^{\mu\nu} \right. \\ & - f_Q \sqrt{-g} (P_{\mu\lambda\xi} Q_{\nu}^{\lambda\xi} - 2Q_{\mu}^{\lambda\xi} P_{\lambda\xi\nu}) \delta g^{\mu\nu} + 2f_Q \sqrt{-g} P_{\lambda\mu\nu} \nabla^{\lambda} \delta g^{\mu\nu} \\ & \left. - \kappa T_{\mu\nu} \sqrt{-g} \delta g^{\mu\nu} \right] d^4 x. \end{aligned} \quad (28)$$

After equating the variation of this equation to zero, the field equations of the $f(Q, T)$ gravity turn out to be

$$\begin{aligned} T_{\mu\nu} = & \frac{-2}{\sqrt{-g}} \nabla_{\lambda} (f_Q \sqrt{-g} P_{\mu\nu}^{\lambda}) - \frac{1}{2} f g_{\mu\nu} + f_T (T_{\mu\nu} + \Theta_{\mu\nu}) \\ & - f_Q (P_{\mu\lambda\xi} Q_{\nu}^{\lambda\xi} - 2Q_{\mu}^{\lambda\xi} P_{\lambda\xi\nu}), \end{aligned} \quad (29)$$

where f_T represents the derivative corresponding to the trace of the energy-momentum tensor and f_Q defines the derivative with respect to non-metricity. Equation (29) represents the field equations in the context of the $f(Q, T)$ theory, and the solution of these equations can provide insights into how gravity behaves in this modified framework.

3 Field Equations and Karmarkar Condition

We consider the inner region as

$$ds^2 = dt^2 e^{\alpha(r)} - dr^2 e^{\beta(r)} - d\theta^2 r^2 - d\phi^2 r^2 \sin^2 \theta. \quad (30)$$

The stress-energy tensor manifests configurations of matter and energy in a system and its components yield physical features that produce distinct aspects of its dynamics. We consider anisotropic matter distribution as

$$T_{\mu\nu} = U_{\mu} U_{\nu} \rho + V_{\mu} V_{\nu} p_r - p_t g_{\mu\nu} + U_{\mu} U_{\nu} p_t - V_{\mu} V_{\nu} p_t, \quad (31)$$

where four-vector and four-velocity of the fluid are denoted by V_μ and U_μ , respectively. In the context of gravitational physics, the matter-Lagrangian density is a fundamental concept that describes the distribution of matter and its dynamics in a given spacetime. We consider matter-Lagrangian density for anisotropic matter as $Lm = -\frac{pr+2pt}{3}$ [68]. This Lagrangian density has been employed in various theoretical models and has shown reasonable success in explaining observations and phenomena involving anisotropic matter distributions, especially in the context of CSs and certain cosmological scenarios. The corresponding field equations turn out to be

$$\begin{aligned} \varrho &= \frac{1}{2r^2e^\beta} \left[2rQ'f_{QQ}(e^\beta - 1) + f_Q((e^\beta - 1)(2 + r\alpha') + (e^\beta + 1)r\beta') \right. \\ &\quad \left. + fr^2e^\beta \right] - \frac{1}{3}f_T(3\varrho + p_r + 2p_t), \end{aligned} \quad (32)$$

$$\begin{aligned} p_r &= \frac{-1}{2r^2e^\beta} \left[2rQ'f_{QQ}(e^\beta - 1) + f_Q((e^\beta - 1)(2 + r\alpha' + r\beta') - 2r\alpha') \right. \\ &\quad \left. + fr^2e^\beta \right] + \frac{2}{3}f_T(p_t - p_r), \end{aligned} \quad (33)$$

$$\begin{aligned} p_t &= \frac{-1}{4re^\beta} \left[-2rQ'\alpha'f_{QQ} + f_Q(2\alpha'(e^\beta - 2) - r\alpha'^2 + \beta'(2e^\beta + r\alpha') \right. \\ &\quad \left. - 2r\alpha'') + 2fre^\beta \right] + \frac{1}{3}f_T(p_r - p_t). \end{aligned} \quad (34)$$

When dealing with multivariate functions and their derivatives, the resulting field equations become more intricate, making it challenging to derive specific outcomes. Consequently, to facilitate analysis, we opt for a particular model of $f(Q, T)$ as [69]

$$f(Q, T) = \gamma Q + \eta T, \quad (35)$$

where γ and η are arbitrary constants.

The key features of this model lie in its departure from the standard Einstein-Hilbert action, allowing for a more comprehensive description of gravitational interactions. By incorporating the trace of the stress-energy tensor, the theory captures non-trivial effects arising from the energy-momentum distribution, which is particularly relevant in the context of CSs where extreme densities and pressures prevail. The assumptions underlying this model include the validity of the Einstein equivalence principle, the existence of a

metric theory and the requirement of covariance under general coordinate transformations. These assumptions enable the formulation of field equations governing the dynamics of matter and geometry in the framework of $f(Q, T)$ gravity. The implications of employing the $f(Q, T)$ theory in our study manifest in the altered field equations and subsequently in the behavior of matter and geometry in CSs. Specifically, deviations from the predictions of EGTR arise in regions of high energy density, impacting the structure and properties of CSs. Therefore, by elucidating the specific model and its implications, we aim to provide a clearer understanding of the interplay between gravitational interactions and the properties of CSs in the framework of $f(Q, T)$ gravity. The considered cosmological model has been widely used in the literature [70].

This model of the $f(Q, T)$ theory emerges as a crucial endeavor in the realm of theoretical physics, particularly in the pursuit of understanding the fundamental nature of physical phenomena at both macroscopic and microscopic scales. Motivated by the quest for a unified framework that can elegantly encapsulate diverse phenomena spanning from cosmology to particle physics, the corresponding model of $f(Q, T)$ theory aims to provide a comprehensive and insightful description of the universe's behavior. One of the primary motivations behind the development of this model lies in addressing the limitations and gaps present in existing theoretical frameworks such as EGTR and quantum mechanics. While these theories have been remarkably successful in explaining various aspects of the universe, they encounter challenges when confronted with scenarios involving extreme conditions or unexplored domains, such as the early universe or black hole singularities.

This model allows for the incorporation of additional degrees of freedom and geometric structures, thereby enabling a more nuanced description of gravitational interactions and their interplay with matter and energy. Furthermore, the minimal model of $f(Q, T)$ theory is motivated by its potential to reconcile discrepancies observed between theoretical predictions and experimental observations. By refining the mathematical formalism and introducing novel dynamical mechanisms, this framework aims to provide more accurate predictions for phenomena such as dark energy, dark matter and gravitational waves, which remain enigmatic in the current theoretical paradigm. Moreover, the quest for a minimal model of $f(Q, T)$ theory is intrinsically linked to broader theoretical endeavors, including the quest for a theory of quantum gravity and the exploration of the fundamental nature of spacetime itself. By probing the intricate interplay between geometry

and matter in the context of $f(Q, T)$ theory, researchers hope to uncover deeper insights into the fabric of the universe and its underlying symmetries. The motivation behind this model of $f(Q, T)$ theory stems from its potential to overcome existing theoretical limitations, reconcile theoretical predictions with experimental observations and provide a more comprehensive understanding of the fundamental laws governing the universe. By embracing this framework, physicists embark on a journey towards unraveling the mysteries of the cosmos and unlocking the secrets of nature at its most fundamental level.

The resulting modified field equations are

$$\varrho = \frac{\gamma e^{-\beta}}{12r^2(2\eta^2 + \eta - 1)} \left[\eta(2r(-\beta'(r\alpha' + 2) + 2r\alpha'' + \alpha'(r\alpha' + 4)) - 4e^\beta + 4) + 3\eta r(\alpha'(4 - r\beta' + r\alpha') + 2r\alpha'') + 12(\eta - 1)(r\beta' + e^\beta - 1) \right], \quad (36)$$

$$p_r = \frac{\gamma e^{-\beta}}{12r^2(2\eta^2 + \eta - 1)} \left[2\eta(r\beta'(r\alpha' + 2) + 2(e^\beta - 1) - r(2r\alpha'' + \alpha'(r\alpha' + 4))) + 3(r(\eta\beta'(r\alpha' + 4) - 2\eta r\alpha'' - \alpha'(-4\eta + \eta r\alpha' + 4)) - 4(\eta - 1) \times (e^\beta - 1)) \right], \quad (37)$$

$$p_t = \frac{\gamma e^{-\beta}}{12r^2(2\eta^2 + \eta - 1)} \left[2\eta(r\beta'(r\alpha' + 2) + 2(e^\beta - 1) - r(2r\alpha'' + \alpha'(r\alpha' + 4))) + 3(r(2(\eta - 1)r\alpha'' - ((\eta - 1)r\alpha' - 2)(\beta' - \alpha')) + 4\eta(e^\beta - 1)) \right]. \quad (38)$$

The well-known Karmarkar condition is defined as [71]

$$R_{1414}R_{2323} = R_{1212}R_{3434} + R_{1224}R_{1334}, \quad (39)$$

where

$$R_{1414} = -\frac{1}{4}(2\alpha'' + \alpha'^2 - \alpha'\beta')e^\alpha, \quad R_{2323} = \frac{1}{e^\beta}r^2 \sin^2 \theta (e^\beta - 1),$$

$$R_{3434} = \frac{-1}{2}r^2 \sin^2 \theta \alpha' e^{\alpha-\beta}, \quad R_{1212} = \frac{1}{2}r\beta', \quad R_{1334} = R_{1224} \sin^2 \theta = 0.$$

This condition was formulated by the Indian mathematician and physicist Shanti Swarup Karmarkar in the 1940s. Its applications extend to diverse

fields, including the derivation of precise solutions, exploration of singularity theorems and the study of cosmological models. It is crucial to recognize that this condition serves as a mathematical instrument for comprehending specific properties of spacetime. It is a geometric condition that involves the Riemann curvature tensors, which characterize the curvature of spacetime. This condition plays a crucial role in understanding the behavior of spacetime in the presence of matter and energy. This constraint has been extensively explored in various contexts such as exact solutions and cosmological models. It is essential to recognize that the Karmarkar condition serves as a specific mathematical tool, facilitating the comprehension of certain spacetime properties. This condition is expressed mathematically as an equation that relates the metric coefficients in the four-dimensional spacetime to certain parameters in the higher-dimensional space. The application of the Karmarkar condition is a technique to generate solutions for the metric functions describing the geometry of a CS. Once these solutions are obtained, further analysis is performed to assess the physical properties of the CSs such as their stability and the matter content required to sustain it. It is important to note that the Karmarkar condition is an approach among various methods used to study CSs and gravitational solutions. The motivation for considering the Karmarkar condition in stellar structure lies in its ability to provide insights into the stability of stars. By analyzing this condition, astronomers can assess whether a star's structure will remain stable over time or if it's prone to instabilities that could lead to phenomena like collapse or disruption.

The Karmarkar condition provides a valuable framework for understanding the equilibrium conditions in stellar interiors, particularly in the context of gravitational collapse and stability analysis. By incorporating the Karmarkar condition into our analysis, we aim to enhance our understanding of the physical processes governing stellar evolution and structure. Specifically, the advantage of considering this condition lies in its ability to provide insights into the internal pressure-density distribution and the overall stability of stellar configurations. Furthermore, the Karmarkar condition offers a rigorous mathematical framework for exploring the behavior of compact astrophysical objects such as white dwarfs, neutron stars and black holes, under extreme conditions of gravitational pressure. By elucidating the implications of this condition on stellar models, we can better constrain theoretical predictions and refine our interpretations of observational data. Thus, the Karmarkar condition provides a valuable tool for studying the stability of

stellar structures, helping astronomers better understand the dynamics and evolution of stars. A lot of work based on the Karmarkar condition in the framework of different modified theories has been done in [72]-[80].

Solving Eq.(39), we obtain

$$\alpha'(\beta' - \alpha') - 2\alpha'' = \frac{\alpha'\beta'}{1 - e^\beta}, \quad (40)$$

where $e^\beta \neq 1$. Integrating this equation, we have

$$e^{\alpha(r)} = (c + d \int \sqrt{e^\beta - 1} dr)^2. \quad (41)$$

Here, the integration constants are denoted by c and d . Further, we choose the metric potential e^β as [81]

$$e^{\beta(r)} = 1 + (1 + br^2)^\lambda a^2 r^2, \quad (42)$$

where one can select λ as any real number except zero. In the framework of EGTR, Singh and Pant [82] considered positive values of λ to analyze the physical characteristics of compact stellar objects. Later, Bhar et al [81] examined this metric element with $\lambda = -4$ and discovered stable cosmic objects. Inspired by their work, we aim to extend the analysis in the context of $f(Q, T)$ gravity by choosing $\lambda = -4$. However, we attempted other choices of λ (both positive and negative) but could not obtain viable results in these cases.

By manipulating Eqs.(41) and (42), we obtain

$$e^{\alpha(r)} = \left(c - \frac{ad}{2b(1 + br^2)} \right)^2. \quad (43)$$

The unknown constants (a, b, c, d) can be found using the first Darmois junction condition. This condition matches interior and exterior spacetimes at the hypersurface. By imposing this condition, researchers can model the behavior of matter in celestial objects, leading to a deeper understanding of their physical properties. We consider the outer geometry of the CSs as

$$ds_+^2 = dt^2 \left(1 - \frac{2m}{r} \right) - dr^2 \left(1 - \frac{2m}{r} \right)^{-1} - d\theta^2 r^2 - d\phi^2 r^2 \sin^2 \theta. \quad (44)$$

Table 1: Approximate values of input parameters.

Compact stars	M_{\odot}	$\mathcal{R}(km)$
4U 1538-52 [83]	0.87 ± 0.07	7.866 ± 0.21
SAX J1808.4-3658 [84]	0.9 ± 0.3	7.951 ± 1.0
Her X-1 [85]	0.85 ± 0.15	8.1 ± 0.41
LMC X-4 [83]	1.04 ± 0.09	8.301 ± 0.2
EXO 1785-248 [86]	1.30 ± 0.2	10.10 ± 0.44

The continuity of metric coefficients of the metrics (30) and (44) at the surface boundary ($r = \mathcal{R}$) gives

$$g_{tt} = 1 + \frac{a^2 r^2}{(1 + br^2)^4} = 1 - \frac{2m}{\mathcal{R}}, \quad (45)$$

$$g_{rr} = \left(c - \frac{ad}{2b(1 + br^2)} \right)^2 = \left(1 - \frac{2m}{\mathcal{R}} \right)^{-1}, \quad (46)$$

$$g_{tt,r} = \frac{2adr \left(c - \frac{ad}{2b(1 + br^2)} \right)}{(1 + br^2)^2} = \frac{2m}{\mathcal{R}^2}. \quad (47)$$

By solving the above equations simultaneously, we obtain

$$a = \frac{(1 + b\mathcal{R}^2)^2}{\mathcal{R}} \left(\frac{2m}{\mathcal{R} - 2m} \right)^{1/2}, \quad (48)$$

$$b = \frac{(4m - \mathcal{R})}{\mathcal{R}^2(9\mathcal{R} - 20m)}, \quad (49)$$

$$c = \frac{ad}{2b(1 + b\mathcal{R}^2)} + \left(1 - \frac{2m}{\mathcal{R}} \right)^{1/2}, \quad (50)$$

$$d = \frac{1}{2\mathcal{R}} \left(\frac{2m}{\mathcal{R}} \right)^{1/2}. \quad (51)$$

The Karmarkar solutions describe the gravitational field around CSs. These solutions involve integration constants that provide essential insights into the gravitational and physical properties of CSs, aiding in the understanding of their structure. These solutions describe the distribution of energy in the CSs. For example, in the case of a neutron star, it provides insight into how the energy is distributed in the interior, which is crucial for

Table 2: Approximate values of output parameters.

Compact stars	a	b	c	d
4U 1538-52	0.0780314	-0.000979628	-0.717909	0.0362963
SAX J1808.4-3658	0.0788571	-0.000929059	-0.821585	0.0363264
Her X-1	0.072303	-0.000983907	-0.517508	0.0343333
LMC X-4	0.0833349	-0.000714639	-1.45075	0.0366062
EXO 1785-248	0.0704159	-0.000454051	-1.6917	0.0304946

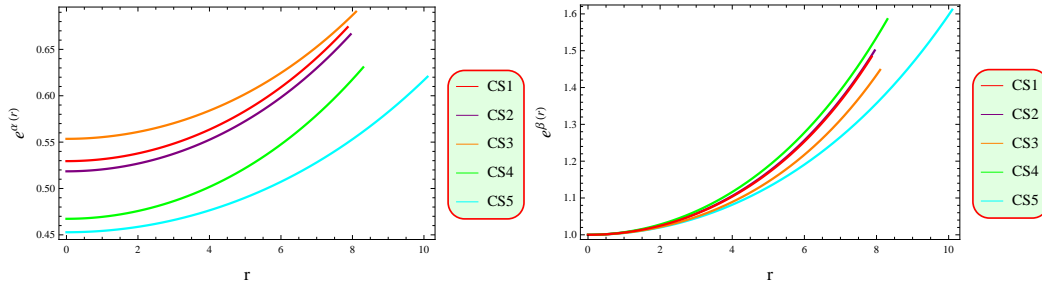


Figure 1: Graphs of metric potential versus radial coordinate.

understanding its stability and structural properties. The solutions can be used to understand gravitational redshift effects near the surface of CSs. Due to the intense gravitational field, electromagnetic radiation emitted from the surface experiences a significant redshift as it travels away from the objects. Depending on the integration constants of the Karmarkar solutions, it may contain features such as event horizons and singularities. These features are indicative of the formation of black holes under certain conditions, providing insight into the final stages of stellar collapse. Thus, the integration constants in Karmarkar solutions offer a theoretical framework for studying the gravitational effects and structural properties of compact stellar objects. Their physical interpretation provides valuable insights into the nature of these objects and their observable characteristics.

Table **1** presents the observed values of mass and radius for the considered CSs, while Table **2** contains the corresponding constants associated with mass and radius. The solution's compatibility is guaranteed by the non-singular and positively increasing behavior of metric elements across the entire domain. Figure **1** determine the behavior of metric potentials, confirming the regularity and necessary positive increase of both metric elements. In the graphs, the abbreviations CS1, CS2, CS3, CS4, and CS5 refer to 4U 1538-52, SAX J1808.4-3658, Her X-1, LMC X-4, and EXO 1785-248 CSs, respectively. The corresponding field equations are

$$\begin{aligned}
\rho &= -a\gamma \left[10bd(br^2 - 3)(1 + br^2)^6\eta + a^4 dr^2(2\eta - 3) - 2a^3 cbr^2(1 + br^2) \right. \\
&\times (2\eta - 3) + 2acb(1 + br^2)^4(5br^2 - 3)(2\eta - 3) - 3a^2 d(br^2 + 1)^3(3 - 2\eta \\
&\left. + 5br^2(2\eta - 1)) \right] \left[3(-ad + 2cb(1 + br^2))(a^2 r^2 + (1 + br^2)^4)^2(1 + \eta) \right. \\
&\left. \times (2\eta - 1) \right]^{-1}, \tag{52}
\end{aligned}$$

$$\begin{aligned}
p_r &= -a\gamma \left[a^4 r^2 d(3 - 2\eta) + 2a^3 cbr^2(1 + br^2)(2\eta - 3) - 3a^2 d(1 + br^2)^3 \right. \\
&\times (-1 - 2\eta + 5br^2(2\eta - 1)) - 2bd(1 + br^2)^6(-3(2 + \eta) + br^2(17\eta - 6)) \\
&\left. + 2acb(1 + br^2)^4(-3 - 6\eta + br^2(26\eta - 3)) \right] \left[3(-ad + 2cb(1 + br^2))(a^2 r^2 \right. \\
&\left. + (1 + br^2)^4)^2(1 + \eta)(2\eta - 1) \right]^{-1}, \tag{53}
\end{aligned}$$

$$\begin{aligned}
p_t = & -a\gamma \left[4a^4 dr^2 \eta - 8a^3 cbr^2(1 + br^2)\eta + 3a^2 d(1 + br^2)^3(1 + 2\eta + br^2 \right. \\
& \times (2\eta - 1)) + 2acb(1 + br^2)^4(-3 - 6\eta + br^2(9 + 2\eta)) + 2bd(1 + br^2)^6 \\
& \times (3(2 + \eta) + br^2(7\eta - 6)) \left. \right] \left[3(2cb - ad(1 + br^2))(a^2 r^2 + (1 + br^2)^4)^2 \right. \\
& \times (1 + \eta)(2\eta - 1) \left. \right]^{-1}. \tag{54}
\end{aligned}$$

4 Viable Features of Compact Stars

In this section, we analyze the viable characteristics of CSs and examine their behavior graphically. Our investigation delves into the influence of various physical parameters such as material variables, energy constraints, EoS parameters, mass, compactness, redshift, equilibrium state (as governed by the Tolman-Oppenheimer equation) and stability analysis (in terms of sound speed and adiabatic index) through graphical representations.

4.1 Energy Density and Pressure Components

The study of fluid variables such as energy density, radial pressure and tangential pressure in self-gravitating stellar objects is crucial for understanding their internal structure. These variables are expected to maximum at the core due to the dense profile of these objects. The positive behavior counteracts the gravitational force, providing support against collapse. Figures **2-3** represent the graphical representation of fluid parameters and their derivatives for each star candidate. These characteristics reach their maximum at the center and exhibit a positive decrease, indicating a highly compact profile for the proposed CSs. Additionally, the radial pressure in each candidate consistently decreases as the radial coordinate increases, ultimately vanishing at the boundary. Figure **3** further demonstrates that the derivative of fluid parameters is zero at the center, turning negative, thus confirming the presence of a highly compact configuration in the context of $f(Q, T)$ theory.

Pressure anisotropy ($\Delta = p_t - p_r$) refers to the phenomenon where pressure in a system is not uniform in all directions. In other words, the pressure can vary depending on the direction in which it is measured. Positive

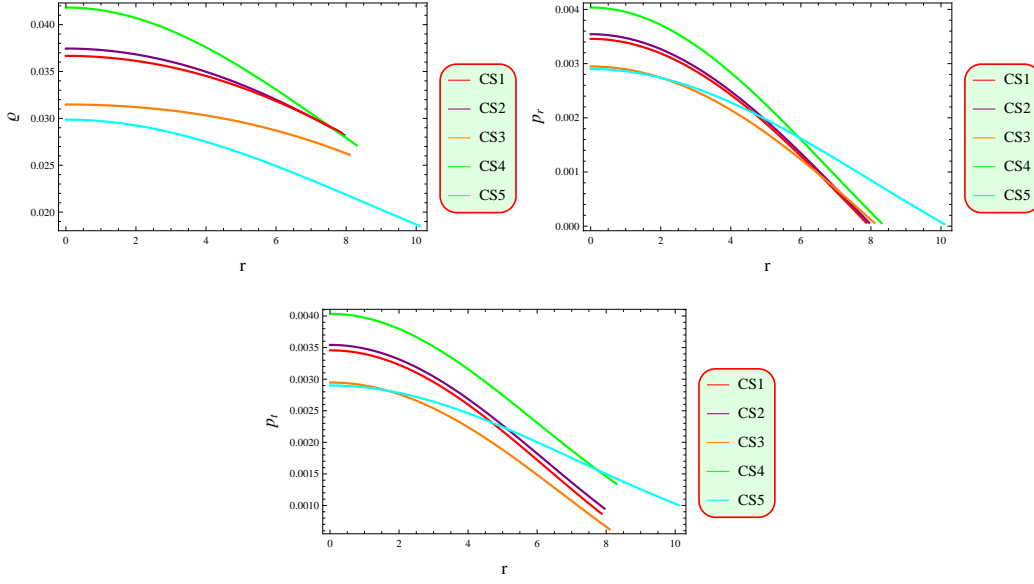


Figure 2: Evolution of matter contents versus radial coordinate.

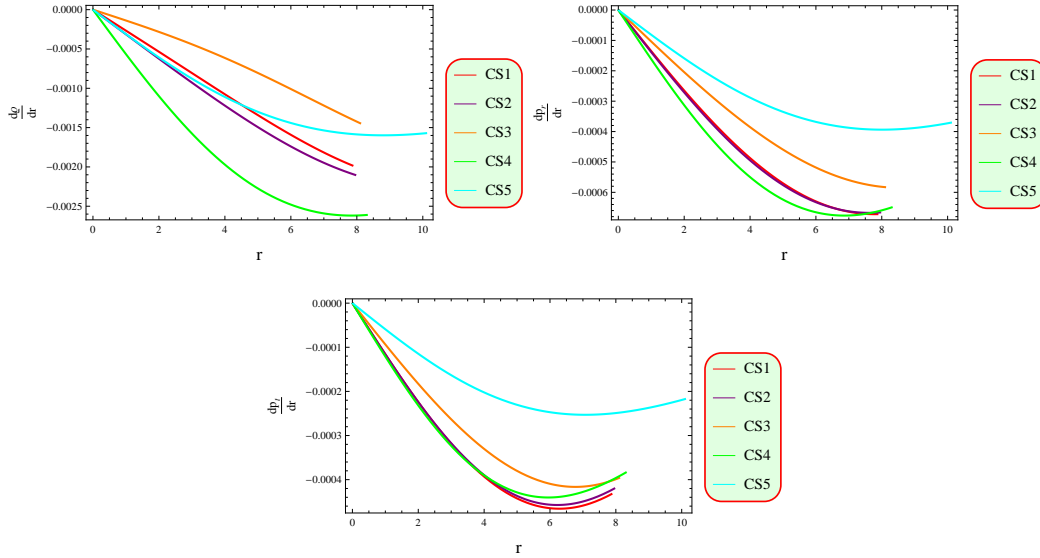


Figure 3: Evolution of gradient of matter contents versus radial coordinate.

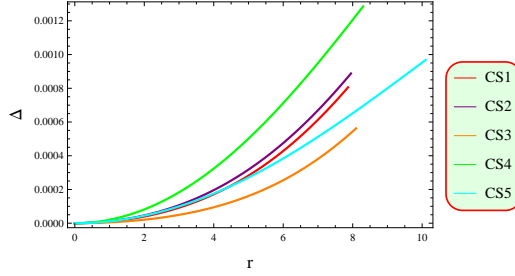


Figure 4: Behavior of $p_t - p_r$ versus radial coordinate.

anisotropy implies outward pressure, while negative anisotropy signifies inward pressure. Figure 4 shows the anisotropic behavior of the proposed CSs. The depicted trend reveals a consistent increase in anisotropy for all CSs, indicating the presence of a repulsive force essential for substantial geometries [87].

4.2 Analysis of Normal Matter

To explore the presence of feasible cosmic structures, it is essential to impose particular constraints on matter, referred to as energy conditions. These conditions encompass a series of inequalities that set limitations on the stress-energy tensor, governing the behavior of matter and energy under the influence of gravity. Various energy conditions exist, each imposing distinct restrictions on the fluid parameters as

- Null energy constraint

$$0 \leq p_r + \varrho, \quad 0 \leq p_t + \varrho.$$

- Dominant energy constraint

$$0 \leq \varrho \pm p_r, \quad 0 \leq \varrho \pm p_t.$$

- Weak energy constraint

$$0 \leq p_r + \varrho, \quad 0 \leq p_t + \varrho, \quad 0 \leq \varrho.$$

- Strong energy constraint

$$0 \leq p_r + \varrho, \quad 0 \leq p_t + \varrho, \quad 0 \leq p_r + 2p_t + \varrho.$$

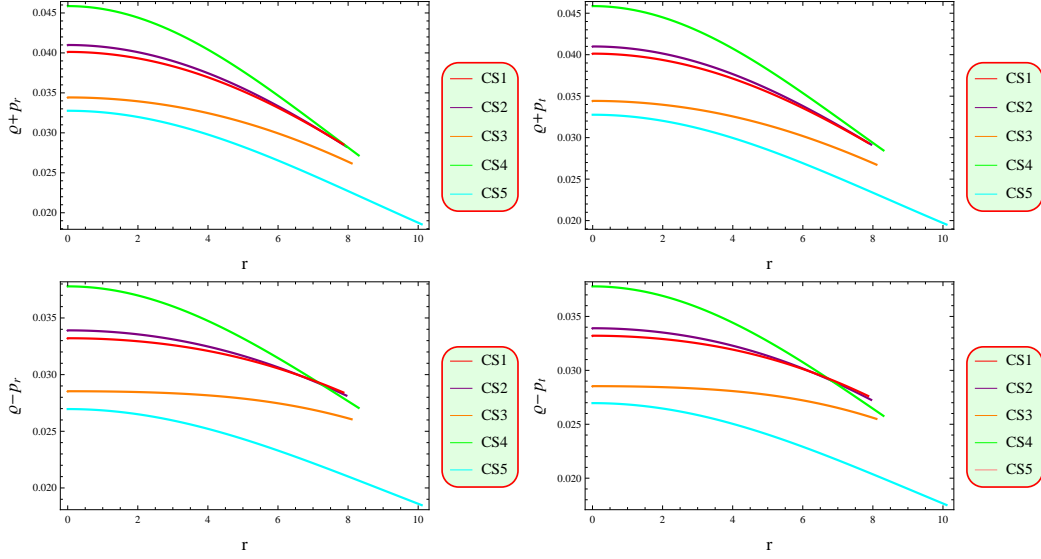


Figure 5: Behavior of energy conditions versus radial coordinate.

Viable cosmic structures must satisfy these conditions. By studying the energy conditions, one can gain insights into the nature of matter and energy, the viability of cosmic structures and the possibilities of phenomena beyond our current understanding of physics. Figure 5 demonstrates that matter inside the cosmic structures is ordinary as all the energy constraints are satisfied in the presence of $f(Q, T)$ terms.

4.3 Analysis of State Parameters

Here, we investigate the equation of state parameters that are crucial in describing the relation between pressure and energy density in various physical systems. The radial ($\omega_r = \frac{p_r}{\rho}$) and transverse ($\omega_t = \frac{p_t}{\rho}$) components must lie in $[0,1]$ for a physically viable model [88]. Using Eqs.(52)-(54), we have

$$\begin{aligned}
\omega_r = & \left[a^4 dr^2 (3 - 2\eta) + 2a^3 cbr^2 (1 + br^2)(2\eta - 3) - 3a^2 d(1 + br^2)^3 (-1 - 2\eta) \right. \\
& + 5br^2(2\eta - 1) - 2bc(1 + br^2)^6 (-3(2 + \eta) + br^2(17\eta - 6)) + 2acb \\
& \left. \times (1 + br^2)^4 (-3 - 6\eta + br^2(26\eta - 3)) \right] \left[10bd(br^2 - 3)(1 + br^2)^6 \eta \right. \\
& \left. + a^4 dr^2 (2\eta - 3) - 2a^3 cbr^2 (1 + br^2)(2\eta - 3) + 2acb(1 + br^2)^4 (5br^2 - 3) \right]
\end{aligned}$$

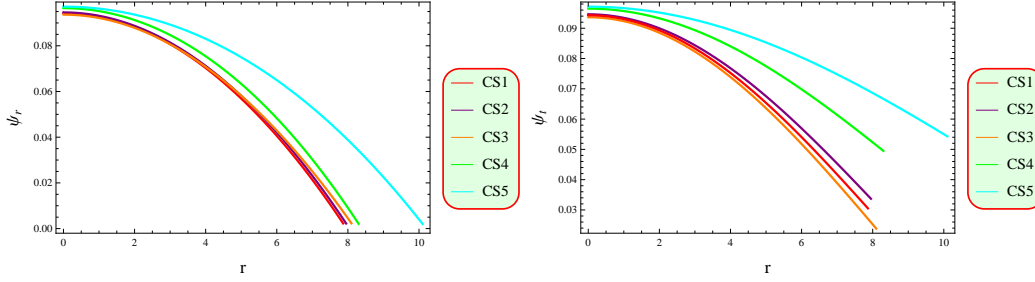


Figure 6: Graphs of radial and tangential components of EoS parameter versus radial coordinate.

$$\begin{aligned}
& \times \left. (2\eta - 3) - 3a^2d(1 + br^2)^3(3 - 2\eta + 5br^2(2\eta - 1)) \right]^{-1}, \\
\omega_t = & \left[4a^4dr^2\eta - 8a^3cbr^2(1 + br^2)\eta + 3a^2d(1 + br^2)^3(1 + 2\eta + br^2(2\eta - 1)) \right. \\
& + 2acb(1 + br^2)^4(-3 - 6\eta + br^2(9 + 2\eta)) + 2bd(1 + br^2)^6(3(2 + \eta) \\
& \left. + br^2(7\eta - 6)) \right] \left[10bd(br^2 - 3)(1 + br^2)^6\eta + a^4dr^2(2\eta - 3) - 2a^3cbr^2 \right. \\
& \times (1 + br^2)(2\eta - 3) + 2acb(1 + br^2)^4(5br^2 - 3)(2\eta - 3) - 3a^2d(1 + br^2)^3 \\
& \left. \times (3 - 2\eta + 5br^2(2\eta - 1)) \right]^{-1}.
\end{aligned}$$

The graphical analysis of EoS parameters is given in Figure 6, which determines that EoS parameters satisfy the required viability condition of the considered CSs.

4.4 Evolution of Different Physical Aspects

The mass of anisotropic CS is defined as

$$M = 4\pi \int_0^{\mathcal{R}} r^2 \rho dr. \quad (55)$$

This equation is numerically solved with the initial condition $M(0) = 0$. Figure 7 manifests the graphical trend of mass distribution in each CS based on this numerical solution. The graph depicts a consistent and positive increase in mass as the radius expands. Moreover, as the radius approaches to 0,

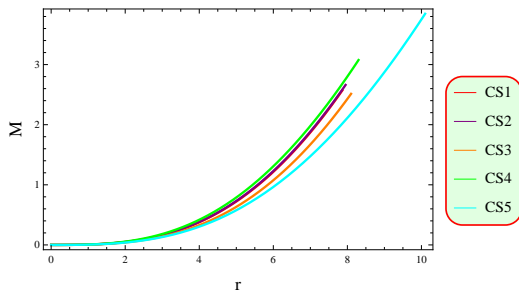


Figure 7: Plots of mass versus radial coordinate.

the mass function converges to 0, indicating a regular behavior at the center of CSs. Analyzing the structural composition of celestial objects involves exploring various physical aspects. One such aspect is the compactness function, denoted as $u = \frac{M}{r}$ which plays a pivotal role in assessing the viability of CSs. Buchdahl [89] introduced a significant limit for the mass-radius ratio, suggesting that viable CSs should satisfy the condition $u < 4/9$.

The surface redshift serves as a crucial parameter for studying the characteristics of CSs, measuring the change in the wavelength of emitted light due to strong gravitational influences. The expression for surface redshift in terms of compactness is given by

$$Z_s = -1 + \frac{1}{\sqrt{1 - 2u}}. \quad (56)$$

Buchdahl [89] established a critical condition stating that the surface redshift must be less than 2 for viable CSs with a perfect matter distribution. However, Ivanov [90] reported a value of 5.211 for anisotropic configurations. Both the compactness and redshift functions exhibit a monotonically increasing behavior, reaching zero at the star's center as shown in Figure 8. It is noteworthy that both functions adhere to specified limits ($u < 4/9$ and $Z_s < 5.211$).

4.5 Mass-Radius and Mass-Inertia Relations

Mass-Radius ($M - R$) and Mass-Inertia ($M - I$) relations are essential tools in the study of CSs. These provide insights into the relationship between mass, radius and moment of inertia for the cosmic objects. The Mass-Radius relationship helps in understanding how the mass of a CS influences its size

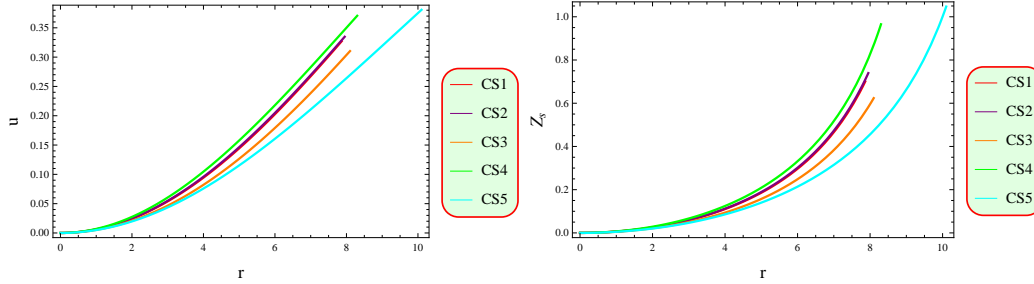


Figure 8: Graphs of compactness factor and surface redshift versus radial coordinate.

and structure. The $M - R$ relation helps astronomers to compare theoretical models with observational data, allowing them to constrain the properties of CSs and understand their internal structure. The $M - I$ shows the relationship between the mass and the moment of inertia of a CS. Moment of inertia is a measure of an object's resistance to changes in rotation. It depends not only on the mass distribution but also on the object's shape and size. In the context of CSs, the $M - I$ relation provides insights into how mass affects the rotational properties of these objects. For example, the neutron stars are known for their rapid rotation. As the mass of a neutron star increases, its moment of inertia also increases, affecting its rotational behavior. The $M - I$ relation is very useful for studying pulsars, which are rapidly rotating neutron stars emitting beams of electromagnetic radiation. By observing the pulsar's rotation period and understanding its moment of inertia, astronomers can infer properties such as its mass and internal structure. Both the Mass-Radius and Mass-Inertia relations are crucial tools for understanding the properties and behavior of CSs, providing valuable insights into the nature of these fascinating objects.

Here, we investigate the gravitational mass and radius with the following condition $e^{-\beta} = 1 - \frac{2M}{R}$. The total mass is obtained as

$$M = \frac{a^2 R^3}{2(a^2 R^2 + (bR^2 + 1)^4)}. \quad (57)$$

The relationship between the total mass (expressed in M_\odot) and the radius (measured in km) is presented graphically in Figure 9. One notable finding from our graphical analysis is the identification of the maximum mass exhibited by a star, which we determine to be 1.3 solar mass. This particular

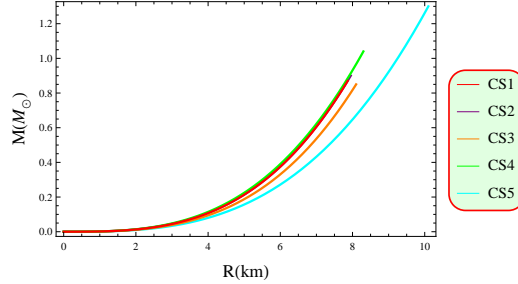


Figure 9: Graph of the total mass corresponding to the total radius.

observation corresponds precisely with existing literature and is consistent with the value provided in Table 1 of our study. Specifically, this maximum mass was associated with the star identified as EXO 1785-248. Such compatibility between our findings and established data reinforces the reliability and validity of our research methodology and results. The study of moment of inertia is crucial in understanding the rotational dynamics of compact objects. In the context of astrophysics, the moment of inertia provides insight into how mass is distributed in an object and how it affects its rotational behavior. Understanding the relationship between mass and moment of inertia is essential for modeling and predicting the behavior of compact objects in astrophysical scenarios, providing valuable insights into their structure and dynamics. The formula for the moment of inertia as suggested by Bejger-Haensel [91]

$$I = \frac{2}{5}(1 + M/M_{\odot})MR^2, \quad (58)$$

allows us to relate the static properties of an object to its rotational characteristics. The maximum mass of a uniformly slow rotating configuration provides an approximate estimation of the moment of inertia. This means that for a given mass and radius, the moment of inertia reaches its maximum value when the object is rotating at its slowest possible rate. Examining the nature of the moment of inertia with respect to mass, it is evident that as mass increases the moment of inertia also increases. This relationship is depicted in Figure 10. As mass increases, the more mass is distributed farther away from the axis of rotation, resulting in a larger moment of inertia. Eventually, the moment of inertia reaches its maximum value for the given mass, indicating that further increases in mass do not significantly affect the rotational dynamics.

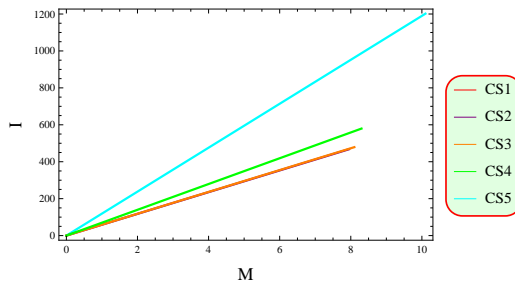


Figure 10: Plot of the moment of inertia with respect to the mass.

5 Equilibrium and Stability Analysis

To Understand the structure and behavior of cosmic objects, it requires a grasp of essential concepts such as equilibrium state and stability analysis. An equilibrium state signifies a balance where internal and external forces acting on cosmic structures are in equilibrium. Stability is critical for assessing the consistency of cosmic structures and involves exploring the conditions under which these structures remain stable against different oscillation modes. This analysis employs the concepts of *sound speed* and *adiabatic index*. Sound speed reflects the speed at which pressure waves propagate through a medium, while the adiabatic index describes the relationship between pressure and density changes in cosmic structures.

5.1 Behavior of Various Forces

Tolman-Oppenheimer equation is a fundamental equation which describes the equilibrium structure of the static spherically symmetric spacetime. It explains how the pressure and gravitational forces of the star are balanced to maintain its equilibrium. This equation describes the balance between the gravitational force pulling the star inward and the pressure exerted by the degenerate fermions or other constituents of the star pushing outward, leading to an equilibrium configuration. In examining the equilibrium state of stellar models, the TOV equation is crucial because it allows astrophysicists to determine the relationship between the pressure, density and mass distribution inside a star. The motivation for exploring the TOV equation in the framework of CSs lies in understanding the theoretical requirements and constraints for the existence of stable CSs. By solving the TOV equation

for various configurations of CSs, we can obtain insights into the behavior of these stars under extreme conditions. Specifically, we investigate the relationship between crucial parameters for understanding their stability and evolution. The TOV equation in the context of CSs contributes to our understanding of the possibilities and limitations of these fascinating constructs in the framework of $f(Q, T)$ theory.

Tolman-Oppenheimer equation for anisotropic matter configuration is [92]

$$\frac{M_G(r)e^{\frac{\alpha-\beta}{2}}}{r^2}(\varrho + p_r) + \frac{dp_r}{dr} - \frac{2}{r}(p_t - p_r) = 0, \quad (59)$$

where

$$M_G(r) = 4\pi \int (\mathbb{T}_t^t - \mathbb{T}_r^r - \mathbb{T}_\theta^\theta - \mathbb{T}_\phi^\phi) r^2 e^{\frac{\alpha+\beta}{2}} dr.$$

Solving this equation, we have

$$M_G(r) = \frac{1}{2} r^2 e^{\frac{\beta-\alpha}{2}} \alpha'.$$

Substituting this value in Eq. (59), we obtain

$$\frac{1}{2} \alpha' (\varrho + p_r) + \frac{dp_r}{dr} - \frac{2}{r} (p_t - p_r) = 0.$$

The resulting solution of this equation offers insights into the star's internal structure, including details about its density profile and pressure distribution. This analysis highlights the impact of gravitational forces ($F_g = \frac{\mu'(\varrho+p_r)}{2}$), hydrostatic forces ($F_h = \frac{dp_r}{dr}$) and anisotropic forces ($F_a = \frac{2(p_r-p_t)}{r}$) on the system. Using Eqs.(52)-(54), we obtain

$$\begin{aligned} F_g &= \left[4bdr(a + abr^2)^2(2bd(1 + br^2)^4 - 2acb(1 + br^2)(3br^2 - 1) + a^2d \right. \\ &\quad \left. \times (5br^2 - 1)\gamma \right] \left[(ad - 2cb(1 + br^2))^2(a^2r^2 + (1 + br^2)^4)^2(1 + \eta) \right]^{-1}, \\ F_a &= \left[2ar(a^2 + 4b(br^2 + 1)^3)(a^2d - 2acb(1 + br^2) + 2bd(1 + br^2)^3)\gamma \right] \\ &\quad \times \left[(-ad + 2cb(1 + br^2))(a^2r^2 + (1 + br^2)^4)^2(\eta + 1) \right]^{-1}, \\ F_h &= \left[2ar\gamma(a^7d^2r^2(2\eta - 3) - 4a^6cbdr^2(1 + br^2)(2\eta - 3) + 8a^2cb^2 \right. \end{aligned}$$

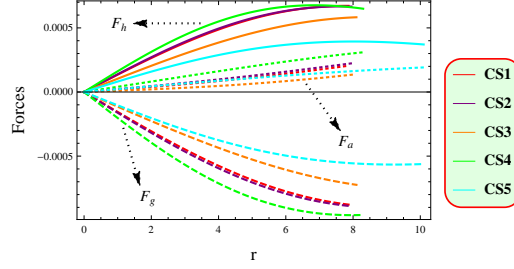


Figure 11: Plot of TOV equation versus radial coordinate.

$$\begin{aligned}
& \times d(1 + br^2)^6(9 + br^2(18 + br^2(9 - 23\eta) - 41\eta) + 32\eta) - 8cb^3d \\
& \times (1 + br^2)^{10}(-6 - 13\eta + br^2(17\eta - 6)) + 2ab^2(1 + br^2)^8((1 + br^2) \\
& \times d^2(-6 - 23\eta + br^2(17\eta - 6)) + 8c^2b(-3 - 14\eta + br^2(26\eta - 3))) \\
& + 4a^4bcd(1 + br^2)^3(3 + 14\eta + br^2(24 - 46\eta + (9 + 40\eta) \\
& \times br^2)) - 2a^3b(1 + br^2)^4(d^2(1 + br^2)(12 + 36\eta + br^2(12 - 59\eta + 25 \\
& \times br^2\eta)) + 2c^2b(3 + 14\eta + br^2(18 - 44\eta + br^2(15 + 38\eta)))) - a^5 \\
& \times (1 + br^2)^2(4c^2b^2r^2(3 - 2\eta) + d^2(3 + 14\eta + br^2(30 - 48\eta + br^2 \\
& \times (46\eta - 9)))) \Big] \left[3(ad - 2cb(1 + br^2))^2(\eta + 2\eta^2 - 1)(a^2r^2 + (1 + br^2)^4)^3 \right]^{-1}.
\end{aligned}$$

Figure 11 shows that our considered CSs are in equilibrium state as the total effect of F_g , F_h and F_a is zero.

5.2 Casuality Condition

The stability analysis of CSs can be examined through the causality condition, ensuring that signals or information do not propagate faster than the speed of light. This criterion dictates that the radial and tangential components of sound speed, denoted as $(u_r = \frac{dp_r}{d\rho})$ and $(u_t = \frac{dp_t}{d\rho})$ must be confined in the interval $[0,1]$ for structures to be considered stable [93]. The expressions for the components of sound speed in the context of $f(Q, T)$ are provided in Appendix C. Figure 12 visually demonstrates that the static spherically symmetric solutions adhere to the required constraints, affirming their stability.

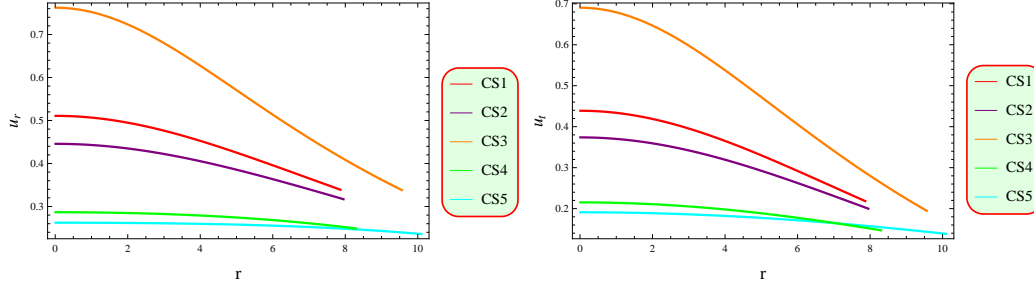


Figure 12: Plots of sound speed versus radial coordinate.

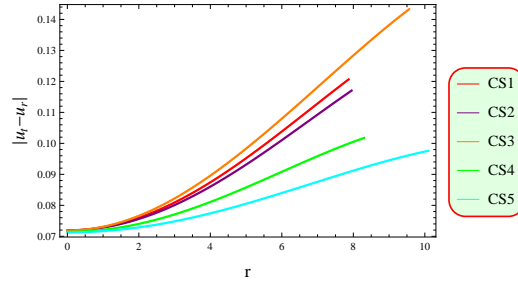


Figure 13: Behavior of Herrera cracking approach.

5.3 Herrera Cracking Approach

The Herrera cracking technique serves as a mathematical tool for examining the stability of solutions. In assessing the stability of CSs, one can evaluate the cracking condition, expressed as $(0 \leq |u_t - u_r| \leq 1)$ [93]. The violation of this cracking condition implies instability, leading to the collapse of CSs. Conversely, the satisfaction of the cracking condition indicates stability, allowing the CSs to persist over an extended period. Figure **13** confirms the stability of the considered CSs, as they remain in the prescribed limits.

5.4 Adiabatic Index

This technique provides information about how matter responds to changes in pressure and density and can be used to determine whether CSs are stable. The adiabatic index is defined as

$$\Gamma_r = \frac{\varrho + p_r}{p_r} u_r, \quad \Gamma_t = \frac{\varrho + p_t}{p_t} u_t,$$

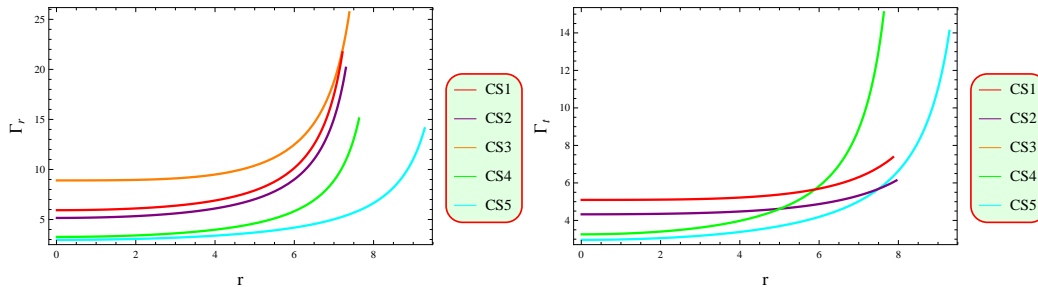


Figure 14: Behavior of adiabatic index versus radial coordinate.

where Γ_r and Γ_t are the radial and tangential components of the adiabatic index. The expressions for Γ_r and Γ_t using Eqs.(52)-(54) are provided in Appendix D. If the value of Γ is less than $4/3$, then CSs are stable, otherwise CSs are unstable and will collapse [94]. Figure 14 shows that our system is stable in the presence of correction terms, as it satisfies the required limit.

6 Conclusions

Modified gravity theories, including $f(Q, T)$ gravity have gained significant attention in recent years as alternative explanations to the EGTR. This theory proposes modification to the fundamental equations of gravity, aiming to address various unresolved questions and challenges in cosmology and astrophysics. One particularly important avenue for testing and constraining this modified gravity theory is through astrophysical observations. Stars, being fundamental objects in the universe which provide an excellent laboratory for investigating the effects of modified gravity. Observations of stars can help us to discern the differences in the behavior of gravity predicted by $f(Q, T)$ theory as compared to EGTR. Stellar properties such as mass, radius, luminosity and evolutionary stages can be affected by modification to the gravitational force law, offering opportunities to test and differentiate between $f(Q, T)$ theory and EGTR. This modified theory often introduces additional free parameters that characterize deviations from EGTR. By studying stars in this theory, we can place constraints on these parameters by comparing theoretical predictions with observed properties of stars, providing valuable insights into the viability of this theory. The study of stars in this modified gravity contributes to our understanding of the fundamental nature of gravity

itself. It helps to refine our knowledge of the laws that govern the behavior of matter and energy in the universe and opens avenues for exploring new phenomena that might not be present in EGTR.

Over the past two decades, the study of CSs has captivated the field of theoretical physics. These cosmic objects pose significant challenges to our comprehension of fundamental physical and present unique opportunities to investigate extreme conditions in the theoretical framework. Our research focuses on examining compact stellar structures in the framework of modified $f(Q, T)$ theory, aiming to delve into the mysteries of the universe. This modified theory holds promise in elucidating phenomena associated with the dark universe. Through the exploration of CSs in this theoretical framework, we have unveiled novel gravitational interactions at both galactic and cosmological scales, providing insight into the nature of these components and their impact on stellar structures. The gravity in compact stellar objects reaches its most extreme limits. Therefore, studying these objects in this theory allows us to probe gravity behavior under conditions of high curvature and density. By scrutinizing the behavior of these extreme celestial objects, we have gained valuable insights into the characteristics of CSs, advancing our comprehension of fundamental interactions in the universe. This research stands to revolutionize our understanding of gravity, opening pathways to a deep understanding of the cosmos and the forces shaping it.

The proposed model of $f(Q, T)$ theory in the context of CSs have significant implications for the behavior of matter and geometry. In CSs such as neutron stars or quark stars, the high density and extreme conditions lead to unique physical phenomena. The inclusion of $f(Q, T)$ terms in the gravitational action affect the behavior of matter in these stars. For instance, it can influence the EOS describing the relationship between pressure and density inside the star. This affects the structure and composition of the star. The modified gravitational action lead to deviations from the predictions of EGTR in terms of the spacetime geometry around CSs. The curvature of spacetime as described by the metric tensor is influenced by the additional modified terms. This can result in modifications to the gravitational field equations, affecting the metric components and curvature profiles around the star. Observationally, the effects of this $f(Q, T)$ model on CSs can manifest in various ways. This model offers a promising framework to explore modifications to gravity in the context of CSs. These include theoretical consistency, constraints from observational data and distinguishing the effects of $f(Q, T)$ modifications from other astrophysical phenomena. Thus,

the minimal model of $f(Q, T)$ theory can significantly impact the behavior of matter and geometry in CSs, potentially leading to observable consequences that may provide insights into the nature of gravity and the properties of dense matter in extreme astrophysical environments.

In our study, we have used the matching conditions at the boundary between the interior and exterior spacetimes of CSs to determine the values of the unknown constants. Specifically, we have used boundary conditions derived from the junction conditions, ensuring continuity of the metric potentials and their derivatives across the boundary. By solving the resulting system of equations, we have obtained the values of the unknown constants that satisfy these matching conditions. Regarding the implications of these values for the behavior and properties of CSs, the determined constants play a crucial role in characterizing the spacetime geometry and matter distribution in the stellar interior. The specific values of these constants directly impact the structural and dynamical properties of CSs, including their stability, maximum mass, compactness and overall gravitational behavior. We acknowledge the importance of elucidating this aspect of our methodology and its significance for understanding the behavior of CSs.

We have used the TOV equation to analyze the equilibrium state of the stellar models under consideration. The results obtained from our analysis provide valuable insights into the stability of CSs. Our study contributes to the understanding of the behavior of CSs and their stability under extreme conditions. We believe that the insights gained from our analysis have important implications for astrophysical phenomena. By incorporating modified gravitational theory and the TOV equation, we have explored implications for theoretical physics and the study of spacetime geometry beyond astrophysical scenarios.

The key findings are summarized as follows.

- The metric functions (Figure 1) are consistent and non-singular, ensuring that the spacetime is smooth and free from singularities.
- The behavior of matter contents (Figure 2) is positive and maximum at the center of the CSs, implying that it has a stable core and decreases towards the boundary, making the CSs physically viable. Moreover, the radial pressure vanishes at the surface boundary ($r = \mathcal{R}$), i.e., $p_r(r = \mathcal{R}) = 0$.
- The gradient of matter contents (Figure 3) vanishes at the center of

CSs and then shows negative behavior, presenting a dense picture of the considered CSs.

- The pressure components are equal at center, which demonstrates that the anisotropy vanishing at the center of CSs. The positive behavior of anisotropy (Figure 4) indicates that pressure is directed outward, which is necessary for CSs.
- All energy constraints (Figure 5) are positive, ensuring the presence of ordinary matter in the interior of CSs, which is necessary to obtain viable CSs.
- The EoS parameters (Figure 6) satisfy the required constraints, i.e., $0 < \omega_r, \omega_t < 1$, which shows the viability of the considered model.
- We have found that the mass function (Figure 7) is regular at the center of CSs and shows a monotonically increasing behavior as the radial coordinate increases.
- The compactness factor is less than $4/9$, and the redshift is less than 5.2, leading to viable CSs structures (Figure 8).
- The graphical behavior of $M - R$ and $M - I$ relations are given in Figures 9 and 10
- Tolman-Oppenheimer equation (Figure 11) shows that all forces (gravitational, hydrostatic, and anisotropic) have a null impact for all proposed CSs. This suggests that the CSs are in an equilibrium state.
- The stability limits i.e. causality condition, Herrera cracking approach and adiabatic index are satisfied ensuring the existence of physically stable CSs (Figures 12-14).

Salako et al [95] studied the existence of strange stars in the background of $f(\mathbb{T}, \mathbb{T})$ gravity, where \mathbb{T} is the torsion tensor. They examined the compact spherical structure of only LMC X-4 strange star candidate using conformal Killing vectors and ensures their stability through several physical parameters. Das et al [96] obtained a new class of interior solutions to the Einstein field equations for an anisotropic matter distribution using a linear EoS. They verified the physical acceptability of the solutions by the current estimated data of pulsar 4U-160852. In contrast, our study diverges by adopting the

$f(Q, T)$ theory, a different theoretical framework that allows for a comprehensive exploration of the effects of modified terms on the viability and stability of CSs. Using distinct methodologies and techniques, we have analyzed several anisotropic CSs, discerning their viability and stability under the influence of modified gravitational dynamics. Our findings reveal the feasibility of the proposed CSs even in the presence of modified terms, underscoring the robustness of our theoretical framework. By expanding the scope of our investigation to encompass a broader spectrum of CSs, we contribute to the ongoing discourse on the behavior of CSs in alternative gravitational theory, thus enriching our understanding of astrophysical phenomena across diverse theoretical landscapes.

We have checked whether our system remains in stable state or not in the presence of $f(Q, T)$ terms. It is found that in the presence of modified terms our system remains in a stable state. Our investigation into the physical aspects has revealed a dense profile of CSs. We have analyzed various essential physical parameters such as metric potentials, effective matter variables, energy conditions, mass, compactness, redshift function, TOV equation, sound speed and adiabatic index, which characterize the stellar system. It is worthwhile to mention here that all these parameters meet the necessary conditions, indicating the presence of viable and stable CSs in this modified framework. Furthermore, the chosen factors for assessing the feasibility and stability of the solution have satisfied their specified limits. Notably, we observed that all parameters reach their maximum values when compared to EGTR and other modified gravitational theories. In the realm of $f(R)$ theory, the results indicate the instability of the Her X-1 CS associated with the second gravity model due to the limited range satisfied by the physical quantities [97]. Furthermore, in the framework of $f(R, T^2)$ theory, it is found that CSs are neither physically viable nor stable at the center [98]. In the light of these findings, it can be concluded that all considered CSs exhibit both physical viability and stability at the center in this modified theory. Consequently, our results suggest that viable and stable CSs can exist in this modified theory. Therefore, we conclude that the solutions we have obtained are physically valid, providing stable and viable structures for anisotropic CSs.

Appendix A: Non-Metricity Scalar

According to Eqs.(18) and (19), we have

$$\begin{aligned}
Q &\equiv -g^{\mu\nu}(L_{\xi\mu}^\lambda L_{\nu\lambda}^\xi - L_{\xi\lambda}^\lambda L_{\mu\nu}^\xi), \\
L_{\xi\mu}^\lambda &= -\frac{1}{2}g^{\lambda\varsigma}(Q_{\mu\xi\varsigma} + Q_{\xi\varsigma\mu} - Q_{\varsigma\mu\xi}), \\
L_{\nu\lambda}^\xi &= -\frac{1}{2}g^{\xi\varsigma}(Q_{\lambda\nu\varsigma} + Q_{\nu\varsigma\lambda} - Q_{\varsigma\lambda\nu}), \\
L_{\xi\mu}^\lambda &= -\frac{1}{2}g^{\lambda\varsigma}(Q_{\lambda\xi\varsigma} + Q_{\xi\varsigma\lambda} - Q_{\varsigma\lambda\xi}), \\
&= -\frac{1}{2}(\bar{Q}_\xi + Q_\xi - \bar{Q}_\xi) = -\frac{1}{2}Q_\xi, \\
L_{\mu\nu}^\xi &= -\frac{1}{2}g^{\xi\varsigma}(Q_{\nu\mu\varsigma} + Q_{\mu\varsigma\nu} - Q_{\varsigma\nu\mu}).
\end{aligned}$$

Thus, we have

$$\begin{aligned}
-g^{\mu\nu}L_{\xi\mu}^\lambda L_{\nu\lambda}^\xi &= -\frac{1}{4}g^{\mu\nu}g^{\lambda\varsigma}g^{\xi\varsigma}(Q_{\mu\xi\varsigma} + Q_{\xi\varsigma\mu} - Q_{\varsigma\mu\xi}) \\
&\quad \times (Q_{\lambda\nu\varsigma} + Q_{\nu\varsigma\lambda} - Q_{\varsigma\lambda\nu}), \\
&= -\frac{1}{4}(Q^{\nu\varsigma\lambda} + Q^{\varsigma\lambda\nu} - Q^{\lambda\nu\varsigma}) \\
&\quad \times (Q_{\lambda\nu\varsigma} + Q_{\nu\varsigma\lambda} - Q_{\varsigma\lambda\nu}), \\
&= -\frac{1}{4}(2Q^{\nu\varsigma\lambda}Q_{\varsigma\lambda\nu} - Q^{\nu\varsigma\lambda}Q_{\nu\varsigma\lambda}), \\
g^{\mu\nu}L_{\xi\lambda}^\lambda L_{\mu\nu}^\xi &= \frac{1}{4}g^{\mu\nu}g^{\xi\varsigma}Q_\varsigma(Q_{\nu\mu\varsigma} + Q_{\mu\varsigma\nu} - Q_{\varsigma\nu\mu}), \\
&= \frac{1}{4}Q^\varsigma(2\bar{Q}_\varsigma - Q_\varsigma), \\
Q &= -\frac{1}{4}(Q^{\lambda\nu\varsigma}Q_{\lambda\nu\varsigma} + 2Q^{\lambda\nu\varsigma\lambda}Q_{\varsigma\lambda\nu} \\
&\quad - 2Q^\varsigma\bar{Q}_\varsigma + Q^\varsigma Q_\varsigma).
\end{aligned}$$

According to Eq.(24), we obtain

$$\begin{aligned}
P^{\lambda\mu\nu} &= \frac{1}{4}[-Q^{\lambda\mu\nu} + Q^{\mu\lambda\nu} + Q^{\nu\lambda\mu} + Q^\lambda g^{\mu\nu} \\
&\quad - \bar{Q}^\lambda g^{\mu\nu} - \frac{1}{2}(g^{\lambda\mu}Q^\nu + g^{\lambda\nu}Q^\mu)],
\end{aligned}$$

$$\begin{aligned}
-Q_{\lambda\mu\nu}P^{\lambda\mu\nu} &= -\frac{1}{4}[-Q_{\lambda\mu\nu}Q^{\lambda\mu\nu} \\
&+ Q_{\lambda\mu\nu}Q^{\mu\lambda\nu} + Q^{\nu\lambda\mu}Q_{\lambda\mu\nu} + Q_{\lambda\mu\nu}Q^\lambda g^{\mu\nu} \\
&- Q_{\lambda\mu\nu}\bar{Q}^\lambda g^{\mu\nu} - \frac{1}{2}Q_{\lambda\mu\nu}(g^{\lambda\mu}Q^\nu + g^{\lambda\nu}Q^\mu)], \\
&= -\frac{1}{4}(-Q_{\lambda\mu\nu}Q^{\lambda\mu\nu} + 2Q_{\lambda\mu\nu}Q^{\mu\lambda\nu} + Q^\lambda Q_\lambda - 2\tilde{Q}^\lambda Q_\lambda), \\
&= Q.
\end{aligned}$$

Appendix B: Variation of Non-Metricity Scalar

All the non-metricity tensors are given as

$$\begin{aligned}
Q_{\lambda\mu\nu} &= \nabla_\lambda g_{\mu\nu}, \\
Q^\lambda{}_{\mu\nu} &= g^{\lambda\xi}Q_{\xi\mu\nu} = g^{\lambda\xi}\nabla_\xi g_{\mu\nu} = \nabla^\lambda g_{\mu\nu}, \\
Q_\lambda{}^\mu{}_\nu &= g^{\mu\varsigma}Q_{\lambda\varsigma\nu} = g^{\mu\varsigma}\nabla_\lambda g_{\varsigma\nu} = -g_{\mu\varsigma}\nabla_\lambda g^{\mu\varsigma}, \\
Q_{\lambda\mu}{}^\nu &= g^{\nu\varsigma}Q_{\lambda\mu\varsigma} = g^{\nu\varsigma}\nabla_\lambda g_{\mu\varsigma} = -g_{\mu\varsigma}\nabla_\lambda g^{\nu\varsigma}, \\
Q^{\lambda\mu}{}_\nu &= g^{\mu\varsigma}g^{\lambda\xi}\nabla_\xi g_{\varsigma\nu} = g^{\mu\varsigma}\nabla^\lambda g_{\nu\varsigma} = -g_{\nu\varsigma}\nabla^\lambda g^{\mu\varsigma}, \\
Q^\lambda{}_\mu{}^\nu &= g^{\nu\varsigma}g^{\lambda\xi}\nabla_\xi g_{\mu\varsigma} = g^{\nu\varsigma}\nabla^\lambda g_{\mu\varsigma} = -g_{\mu\varsigma}\nabla^\lambda g^{\nu\varsigma}, \\
Q_\lambda{}^{\mu\nu} &= g^{\mu\varsigma}g^{\nu\xi}\nabla_\lambda g_{\varsigma\xi} = -g^{\mu\varsigma}g_{\varsigma\xi}\nabla_\lambda g^{\nu\varsigma} = -\nabla_\lambda g^{\mu\nu}.
\end{aligned}$$

By using Eq.(25), we have

$$\begin{aligned}
\delta Q &= -\frac{1}{4}\delta(-Q^{\lambda\nu\varsigma}Q_{\lambda\nu\varsigma} + 2Q^{\lambda\nu\varsigma}Q_{\varsigma\lambda\nu} - 2Q^\varsigma\bar{Q}_\varsigma + Q^\varsigma Q_\varsigma), \\
&= -\frac{1}{4}(-\delta Q^{\lambda\nu\varsigma}Q_{\lambda\nu\varsigma} - Q^{\lambda\nu\varsigma}\delta Q_{\lambda\nu\varsigma} + 2\delta Q_{\lambda\nu\varsigma}Q^{\varsigma\lambda\nu} \\
&+ 2Q^{\lambda\nu\varsigma}\delta Q_{\varsigma\lambda\nu} - 2\delta Q^\varsigma\bar{Q}_\varsigma + \delta Q^\varsigma Q_\varsigma - 2Q^\varsigma\delta\bar{Q}_\varsigma + Q^\varsigma\delta Q_\varsigma), \\
&= -\frac{1}{4}[Q_{\lambda\nu\varsigma}\nabla^\lambda\delta g^{\nu\varsigma} - Q^{\lambda\nu\varsigma}\nabla_\lambda\delta g_{\nu\varsigma} - 2Q_{\varsigma\lambda\nu}\nabla^\lambda\delta g^{\nu\varsigma} \\
&+ 2Q^{\lambda\nu\varsigma}\nabla_\varsigma\delta g_{\lambda\nu} + 2\bar{Q}_\varsigma g^{\mu\nu}\nabla^\varsigma\delta g_{\mu\nu} + 2Q^\varsigma\nabla^\xi\delta g_{\varsigma\xi} \\
&+ 2\bar{Q}_\varsigma g_{\mu\nu}\nabla^\varsigma\delta g^{\mu\nu} - Q_\varsigma\nabla^\xi g^{\mu\nu}\delta g_{\mu\nu} - Q_\varsigma g_{\mu\nu}\nabla^\varsigma\delta g^{\mu\nu} \\
&- Q_\varsigma g^{\mu\nu}\nabla_\varsigma\delta g_{\mu\nu} - Q^\varsigma g_{\mu\nu}\nabla_\varsigma\delta g_{\mu\nu}].
\end{aligned}$$

We use the following relations to simplify the above equation

$$\delta g_{\mu\nu} = -g_{\mu\lambda}\delta g^{\lambda\xi}g_{\xi\nu} - Q^{\lambda\nu\varsigma}\nabla_\lambda\delta g_{\nu\varsigma},$$

$$\begin{aligned}
\delta g_{\nu\varsigma} &= -Q^{\lambda\nu\varsigma}\nabla_\lambda(-g_{\nu\mu}\delta g^{\mu\xi}g_{\xi\varsigma}), \\
&= 2Q^{\lambda\nu}_\varsigma Q_{\lambda\nu\mu}\delta g^{\mu\varsigma} + Q_{\lambda\xi\varsigma}\nabla^\lambda g^{\mu\varsigma} \\
&= 2Q^{\lambda\xi}_\nu Q_{\lambda\xi\nu}\delta g^{\mu\nu} + Q_{\lambda\nu\varsigma}\nabla^\lambda g^{\nu\varsigma}, \\
2Q^{\lambda\nu\varsigma}\nabla_\varsigma\delta g_{\lambda\nu} &= -4Q_\mu^{\xi\varsigma}Q_{\varsigma\xi\nu}\delta g^{\mu\nu} - 2Q_{\nu\varsigma\lambda}\nabla^\lambda\delta g^{\nu\varsigma}, \\
-2Q^\varsigma\nabla^\xi\delta g_{\varsigma\xi} &= 2Q^\lambda Q_{\nu\lambda\mu}\delta g^{\mu\nu} + 2Q_\mu\bar{Q}_\nu\delta g^{\mu\nu} \\
&\quad + 2Q_\nu g_{\lambda\varsigma}\nabla^\lambda g^{\nu\varsigma}.
\end{aligned}$$

Thus, we have

$$\delta Q = 2P_{\lambda\nu\varsigma}\nabla^\lambda\delta g^{\nu\varsigma} - (P_{\mu\lambda\xi}Q_\nu^{\lambda\xi} - 2P_{\lambda\xi\nu}Q_\nu^{\lambda\xi})\delta g^{\mu\nu},$$

where

$$\begin{aligned}
2P_{\lambda\nu\varsigma} &= -\frac{1}{4}[2Q_{\lambda\nu\varsigma} - 2Q_{\varsigma\lambda\nu} - 2Q_{\nu\varsigma\lambda} \\
&\quad + 2(\bar{Q}_\lambda - Q_\lambda)g_{\nu\varsigma} + 2Q_\nu g_{\lambda\xi}], \\
4(P_{\mu\lambda\xi}Q_\nu^{\lambda\xi} - 2P_{\lambda\xi\nu}Q_\nu^{\lambda\xi}) &= 2Q^{\lambda\xi}_\nu Q_{\lambda\xi\mu} - 4Q_\mu^{\lambda\xi}Q_{\xi\lambda\nu} + 2Q_{\lambda\mu\nu}\bar{Q}^\lambda \\
&\quad - Q^\lambda Q_{\lambda\mu\nu} + 2Q^\lambda Q_{\nu\lambda\mu} + 2Q_\mu\bar{Q}_\nu.
\end{aligned}$$

Appendix C

The radial and tangential components of sound speed are given by

$$\begin{aligned}
u_{sr} &= \left[a^7 d^2 r^2 (3 - 2\eta) + 4a^6 c b d r^2 (1 + br^2)(2\eta - 3) + 8cb^3(1 + br^2)^{10}d(-6 \right. \\
&\quad - 13\eta + br^2(17\eta - 6)) + 8a^2 cb^2 d(1 + br^2)^6(-9 - 32\eta + br^2(-18 + 41\eta \\
&\quad + br^2(23\eta - 9))) - 2ab^2(1 + br^2)^8(d^2(1 + br^2)(-23\eta - 6 + br^2(17\eta - 6)) \\
&\quad + 8c^2 b(-3 - 14\eta + br^2(26\eta - 3))) - 4a^4 c b d(1 + br^2)^3(3 + 14\eta + br^2(24 \\
&\quad - 46\eta + br^2(9 + 40\eta))) + (1 + br^2)^4 2a^3 b(d^2(1 + br^2)(12 + 36\eta + br^2(12 \\
&\quad - 59\eta + 25br^2\eta)) + 2c^2 b(14\eta + 3 + br^2(18 - 44\eta + br^2(15 + 38\eta)))) \\
&\quad \left. + a^5(1 + br^2)^2(4c^2(3 - 2\eta)b^2 r^2 + d^2(3 + 14\eta + br^2(30 - 48\eta + br^2 \right. \\
&\quad \left. \times (46\eta - 9)))) \right] \left[-40cb^3 d(br^2 - 5)(1 + br^2)^{10}\eta + a^7 d^2 r^2 (2\eta - 3) \right. \\
&\quad - 4a^6 c b r^2 (1 + br^2) d(-3 + 2\eta) + 10ab^2(1 + br^2)^8(d^2(br^2 - 7)(1 + br^2)\eta \\
&\quad \left. - 8c^2 b(br^2 - 1)(2\eta - 3)) + 40a^2 cb^2 d(1 + br^2)^6(6 - 2\eta - br^2\eta + b^2 r^4 \right.
\end{aligned}$$

$$\begin{aligned}
& \times (11\eta - 6)) - 4a^4cbd(1 + br^2)^3(5(-3 + 2\eta) + br^2(6 - 14\eta + br^2 \\
& \times (44\eta - 51))) - 2a^3b(1 + br^2)^4(-2c^2b(5 + (-2 + 17br^2))br^2(2\eta - 3) \\
& + 5d^2(1 + br^2)(6 + br^2(-7\eta + br^2(17\eta - 6)))) + a^5(br^2 + 1 + b(-7\eta \\
& + br^2(17\eta - 6))) + a^5(1 + br^2)^2(4(2\eta - 3)c^2b^2r^2 + d^2(5(2\eta - 3) + br^2 \\
& \times (6 - 24\eta + br^2(74\eta - 51)))) \Big]^{-1}, \\
u_{st} = & \left[2(2a^7d^2r^2\eta - 8a^6c b d r^2(1 + br^2)\eta - 4cb^3d(1 + br^2)^{10}((7\eta - 6)r^2b \right. \\
& + 12 + \eta) + ab^2(1 + br^2)^8[-8c^2b(-6 - 8\eta + br^2(9 + 2\eta)) + d^2(1 + br^2) \\
& \times (18 - \eta + br^2(7\eta - 6)) + 2a^2cb^2d(1 + br^2)^6(-33 - 34\eta + br^2 \\
& \times (24 - 38\eta + br^2(16\eta - 3))) - 2a^4cbd(1 + br^2)^3(6 + 8\eta + br^2(-9 \\
& + 20\eta + br^2(15 + 28\eta))) + a^5(1 + br^2)^2(8c^2b^2r^2\eta + d^2(3 + 4\eta + br^2 \\
& \times (12\eta - 3 + br^2(3 + 8\eta)))) + a^3b(1 + br^2)^4(4c^2b(3 + 4\eta + br^2(-6 \\
& + 8\eta + br^2(9 + 16\eta))) - d^2(1 + br^2)(-3(7 + 6\eta) + br^2(-19\eta + 27 \\
& + br^2(23\eta - 24)))) \Big] \left[-40cb^3d(br^2 - 5)(1 + br^2)^{10}\eta + a^7(2\eta - 3) \right. \\
& \times d^2r^2 - 4a^6c b d r^2(1 + br^2)(2\eta - 3) + 10ab^2(1 + br^2)^8(d^2(br^2 - 7) \\
& \times (1 + br^2)\eta - 8c^2b(br^2 - 1)(2\eta - 3)) + 40a^2c b d^2d(1 + br^2)^6(-2\eta \\
& + 6 + b^2r^4(11\eta - 6) - br^2\eta) - 4a^4cbd((1 + br^2)^3(5(-3 + 2\eta) + br^2 \\
& \times (6 + br^2(44\eta - 51) - 14\eta)) - 2a^3b(1 + br^2)^4(-2c^2b((-2 + 17br^2) \\
& \times br^2 + 5)(-3 + 2\eta) + 5d^2(1 + br^2)(6 + br^2(-7\eta + br^2(-6 + 17\eta)))) \\
& + a^5(1 + br^2)^2(4(2\eta - 3)c^2b^2r^2 + d^2(5(2\eta - 3) + br^2(6 - 24\eta + br^2 \\
& \times (74\eta - 51)))) \Big]^{-1}.
\end{aligned}$$

Appendix D

The radial and tangential components of adiabatic index are given by

$$\begin{aligned}
\Gamma_r = & \left[-6(1 + br^2)^3(2bd(1 + br^2)^4 - 2acb(1 + br^2)(3br^2 - 1) + a^2d \right. \\
& \times (5br^2 - 1))(2\eta - 1)(a^7d^2r^2(3 - 2\eta) + 4a^6c b d r^2(2\eta - 3) \\
& \times (1 + br^2) + 8cb^3d(1 + br^2)^{10}(-6 - 13\eta + br^2(17\eta - 6)) + 8a^2
\end{aligned}$$

$$\begin{aligned}
& \times cb^2d(1+br^2)^6(-9-32\eta+br^2(-18+41\eta+br^2(23\eta-9))) \\
& - 2ab^2(1+br^2)^8(d^2(1+br^2)(-6-23\eta+br^2(17\eta-6))+8c^2b \\
& \times (-3-14\eta+br^2(26\eta-3))) - 4a^4cbd(1+br^2)^3(3+14\eta+br^2 \\
& \times (24-46\eta+br^2(9+40\eta))) + 2a^3b(1+br^2)^4(d^2(1+br^2)(36\eta \\
& + 12+br^2(12-59\eta+25br^2\eta)) + 2c^2b(3+14\eta+br^2(18-44\eta \\
& + br^2(15+38\eta)))) + a^5(1+br^2)^2(4c^2b^2r^2(3-2\eta)+d^2(3+14\eta \\
& + br^2(30-48\eta+br^2(46\eta-9)))) \Big] \Big[(a^4dr^2(2\eta-3) - 2a^3cbr^2 \\
& (1+br^2)(2\eta-3) + 3a^2d(1+br^2)^3(-1-2\eta+5br^2(2\eta-1)) \\
& + 2bd(1+br^2)^6(-3(2+\eta)+br^2(17\eta-6)) - 2acb(1+br^2)^4(-3 \\
& - 6\eta+br^2(26\eta-3)))(a^7d^2r^2(3-2\eta)+40cb^3d(1+br^2)^{10}\eta \\
& \times (br^2-5) + 4a^6cldr^2(1+br^2)(2\eta-3) + 10ab^2(1+br^2)^8 \\
& \times (d^2(7+br^2(6-br^2))\eta + 8c^2b(br^2-1)(2\eta-3)) - 40a^2cb^2d \\
& \times (1+br^2)^6(6-2\eta-br^2\eta+b^2r^4(11\eta-6)) + 4a^4cbd(1+br^2)^3 \\
& \times (5(2\eta-3)+br^2(6-14\eta+br^2(44\eta-51))) + 2a^3b(1+br^2)^4 \\
& \times (-2c^2b(5+br^2(17br^2-2))(2\eta-3) + 5d^2(1+br^2)(6+br^2 \\
& \times (-7\eta+br^2(17\eta-6)))) - a^5(1+br^2)^2(4c^2b^2r^2(2\eta-3) \\
& + d^2(5(2\eta-3)+br^2(6-24\eta+br^2(74\eta-51)))) \Big]^{-1},
\end{aligned}$$

$$\begin{aligned}
\Gamma_t = & \Big[6(a^2d - 2acb(1+br^2) - 2bd(1+br^2)^3)(a^2r^2 - 2(br^2-1) \\
& \times (1+br^2)^3)(2\eta-1)(2a^7d^2r^2\eta - 8a^6cldr^2(1+br^2)\eta - 4cd \\
& \times b^3(1+br^2)^{10}(12+\eta+br^2(7\eta-6)) + ab^2(1+br^2)^8(-8c^2b \\
& \times (-6-8\eta+br^2(9+2\eta)) + d^2(1+br^2)(18-\eta+br^2(7\eta-6))) \\
& \times 2a^2cb^2d(1+br^2)^6(-33-34\eta+br^2(24-38\eta+br^2(16\eta-3))) \\
& - 2a^4cbd(1+br^2)^3(6+8\eta+br^2(-9+20\eta+br^2(15+28\eta))) + a^5 \\
& \times (1+br^2)^2(8c^2b^2r^2\eta + d^2(3+4\eta+br^2(-3+12\eta+br^2(3+8\eta)))) \\
& + a^3b(1+br^2)^4(4c^2b(3+4\eta+br^2(-6+8\eta+br^2(9+16\eta))) - d^2 \\
& \times (1+br^2)(-3(7+6\eta)+br^2(27-19\eta+br^2(23\eta-24)))) \Big] \\
& \times \Big[(4a^4dr^2\eta - 8a^3cbr^2(1+br^2)\eta + 3a^2d(1+br^2)^3(1+2\eta+br^2
\end{aligned}$$

$$\begin{aligned}
& \times (2\eta - 1)) + 2acb(1 + br^2)^4(-3 - 6\eta + br^2(9 + 2\eta)) + 2(1 + br^2)^6 \\
& \times bd(3(2 + \eta) + br^2(7\eta - 6))(-40cb^3d(br^2 - 5)(1 + br^2)^{10}\eta \\
& + a^7d^2r^2(2\eta - 3) - 4a^6cbr^2(1 + br^2)(2\eta - 3) + 10ab^2(1 + br^2)^8 \\
& \times (d^2(br^2 - 7)(1 + br^2)\eta - 8c^2b(br^2 - 1)(2\eta - 3) + 40a^2cb^2d \\
& \times (1 + br^2)^6(6 - 2\eta - br^2\eta + b^2r^4(11\eta - 6)) - 4a^4cdb(1 + br^2)^3 \\
& \times (5(2\eta - 3) + br^2(6 - 14\eta + br^2(44\eta - 51))) - 2a^3b(1 + br^2)^4(-2 \\
& \times c^2b(5 + br^2(17br^2 - 2))(2\eta - 3) + 5d^2(1 + br^2)(6 + br^2(-7\eta \\
& + br^2(17\eta - 6)))) + a^5(1 + br^2)^2(4c^2b^2r^2(2\eta - 3) + d^2(5(2\eta - 3) \\
& + br^2(6 - 24\eta + br^2(74\eta - 51)))))]^{-1}.
\end{aligned}$$

Data Availability Statement: No new data was created or analyzed in this study.

References

- [1] Baade, W. and Zwicky, F.: Phys. Rev. **46**(1934)76.
- [2] Longair, M.S.: *High Energy Astrophysics* (Cambridge Univeristy Press, 1994).
- [3] Dev, K. and Gleiser, M.: Gen. Relativ. Gravit. **39**(2002)1793.
- [4] Mak, M.K. and Harko, T.: Int. J. Mod. Phys. D **13**(2004)156.
- [5] Eisenhart, L.P.: *Riemannian Geometry* (Princeton University Press, 1925).
- [6] Maurya, S.K. et al.: Eur. Phys. J. A **52**(2016)191; Eur. Phys. J. C **76**(2016)266.
- [7] Singh, K.N. and Pant, N.: Eur. Phys. J. C **76**(2016)524.
- [8] Bhar, P. et al.: Int. J. Mod. Phys. D **26**(2017)1750078.
- [9] Weyl, H.S.: Preuss. Akad. Wiss. **1**(1918)465.
- [10] Kirsch, I.: Phys. Rev. **72**(2005)024001; Boulanger, N. and Kirsch, I.: Phys. Rev. **73**(2006)124023.

- [11] Aldrovandi, R. and Pereira, J.G.: *Teleparallel Gravity: An Introduction* (Springer Science and Business Media, 2012).
- [12] Jimenez, J.B., Heisenberg, I. and Koivisto, L.T.: Phys. Rev. **98**(2018)044048.
- [13] Felice, A.D. and Tsujikawa, S.R.: Living Rev. Relativ. **13**(2010)3; Mustafa, G. et al.: Phys. Rev. D **101**(2020)104013; Phys. Scr. **96**(2021)045009; Phys. Dark Universe **31**(2021)100747.
- [14] Gul, M.Z. and Sharif, M.: Chin. J. Phys. **88**(2024)388.
- [15] Gul, M.Z. and Sharif, M.: New Astron. **106**(2024)102137.
- [16] Harko, T., et al.: Phys. Rev. D **84**(2011)024020; Mustafa, G. et al.: Chin. J. Phys. **67**(2020)576; Eur. Phys. J. C **80**(2020)26; Astrophys. J. **941**(2022)170.
- [17] Sharif, M., Gul, M.Z.: Mod. Phys. Lett. A **36**(2021)2150214.
- [18] Gul, M.Z., Sharif, M. and Kanwal, I.: New Astron. **109**(2024)102204.
- [19] Sharif, M., Shakeel, M. and Gul, M.Z.: New Astron. **108**(2024)102179.
- [20] Sharif, M., Gul, M.Z.: Eur. Phys. J. Plus **133**(2018)345.
- [21] Sharif, M., Gul, M.Z.: Chin. J. Phys. **57**(2019)329.
- [22] Sharif, M., Gul, M.Z.: Int. J. Mod. Phys. D **28**(2019)1950054.
- [23] Adeel, M. et al.: Mod. Phys. Lett. A **38**(2023)2350152.
- [24] Gul, M.Z. et al.: Eur. Phys. J. C **84**(2024)8;
- [25] Rani, S. et al.: Int. J. Geom. Methods Mod. Phys. **21**(2024)2450033.
- [26] Crisostomi, M., Koyama, K. and Tasinato, G.: J. Cosmol. Astropart. Phys. **04**(2016)044.
- [27] Xu, Y. et al.: Eur. Phys. J. C **79**(2019)708.
- [28] Arora, S. et al.: Phys. Dark Universe **30**(2020)100664.
- [29] Bhattacharjee, S. and Sahoo, P.K.: Eur. Phys. J. C **80**(2020)289.

- [30] Arora, S. and Sahoo, P.K.: Phys. Scr. **95**(2020)095003.
- [31] Xu, Y., Harko, T., Shahidi, S., and Liang, S.D.: Eur. Phys. J. C **80**(2020)449.
- [32] Najera, A. and Fajardo, A.: Phys. Dark Universe **34**(2021)100889.
- [33] Godani, N. and Samanta, G.C.: Int. J. Geom. Methods Mod. Phys. **18**(2021)2150134.
- [34] Agrawal, A.S., Pati, L., Tripathy, S.K., and Mishra, B.: Phys. Dark Universe **33**(2021)100863.
- [35] Pradhan, S., Mohanty, D. and Sahoo, P.K.: Chin. Phys. C **47**(2023)095104.
- [36] Arapoglu, S., Deliduman, C. and Eksi, K.Y.: J. Cosmol. Astropart. Phys. **07**(2011)020.
- [37] Astashenok, A.V., Capozziello, S. and Odintsov, S.D.: Phys. Rev. D **89**(2014)103509.
- [38] Das, A. et al.: Eur. Phys. J. C **76**(2016)654.
- [39] Deb, D. et al.: J. Cosmol. Astropart. Phys. **2018**(2018)044.
- [40] Biswas, S. et al.: Ann. Phys. **401**(2019)20.
- [41] Bhar, P., Singh, K.N. and Tello-Ortiz, F.: Eur. Phys. J. C **79**(2019)922.
- [42] Sharif, M. and Ramzan, A.: Phys. Dark Universe 30(2020)100737; Astrophys. Space Sci. **365**(2020)137.
- [43] Dey, S., Chanda, A. and Paul, B.C.: Eur. Phys. J. Plus **136**(2021)228.
- [44] Sharif, M. and Gul, M.Z.: Phys. Scr. **96**(2021)025002;
- [45] Sharif, M. and Gul, M.Z.: Phys. Scr. **07**(2021)154.
- [46] Sharif, M. and Gul, M.Z.: Adv. Astron. **2021**(2021)6663502.
- [47] Sharif, M. and Gul, M.Z.: Eur. Phys. J. Plus **136**(2021)503.
- [48] Sharif, M. and Gul, M.Z.: Chin. J. Phys. **80**(2022)58.

- [49] Sharif, M. and Gul, M.Z.: J. Exp. Theor. Phys. **136**(2023)436.
- [50] Gul, M.Z. and Sharif, M.: Symmetry **15**(2023)684.
- [51] Sharif, M. and Gul, M.Z.: Phys. Scr. **96**(2021)105001;
- [52] Sharif, M. and Gul, M.Z.: Pramana J. Phys. **96**(2022)153.
- [53] Sharif, M. and Gul, M.Z.: Universe **9**(2023)145.
- [54] Sharif, M. and Gul, M.Z.: Int. J. Mod. Phys. A **36**(2021)2150004;
- [55] Sharif, M. and Gul, M.Z.: Universe **7**(2021)154.
- [56] Sharif, M. and Gul, M.Z.: Chin. J. Phys. **71**(2021)365.
- [57] Sharif, M. and Gul, M.Z.: Mod. Phys. Lett. A **37**(2022)2250005.
- [58] Sharif, M. and Gul, M.Z.: Int. J. Geom. Methods Mod. Phys. **19**(2022)2250012.
- [59] Sharif, M. and Gul, M.Z.: Gen. Relative. Gravit. **55**(2023)10;
- [60] Sharif, M. and Gul, M.Z.: Phys. Scr. **98**(2023)035030.
- [61] Sharif, M. and Gul, M.Z.: Pramana-J. Phys. **97**(2023)122.
- [62] Mustafa, G. et al.: Phys. Scr. **96**(2021)105008; Chin. J. Phys. **77**(2022)1742; Chin. J. Phys. **67**(2020)576; Phys. Dark Universe **30**(2020) 100652; Phys. Scr. **96**(2021)045009.
- [63] Javed, F. et al.: Nucl. Phys. B **990**(2023)116180; Fortschr. Phys. **2023**(2023)2200214; Eur. Phys. J. C **83**(2023)1088; Javed, F.: Eur. Phys. J. C **83**(2023)513; Ann. of Phys. **458**(2023)169464; Int. J. Geom. Methods. Mod. Phys **19**(2022)2250190.
- [64] Dirac, P.A.M.: Proc. R. Soc. Lond. A **333**(1973)403.
- [65] Novello, M. and Perez Bergliaffa, S.E.: Phys. Rep. **463**(2008)127.
- [66] Hehl, F.W. et al.: Rev. Mod. Phys. **48**(1976)393.
- [67] Landau, L.D. and Lifshitz, E.M.: *The Classical Theory of Fields* (Pergamon Press, Oxford, 1970).

- [68] Moraes, P.H.R.S. and Sahoo, P.K.: Phys. Rev. D **97**(2018)024007; Maurya, S.K. et al.: Phys. Rev. D. **100**(2019)044014; Rahaman, M. et al.: Eur. Phys. J. C **80**(2020)272.
- [69] Xu, Y. et al.: Eur Phys. J. C **80**(2020)449.
- [70] Tayde, M. et al.: Chin. Phys. C **46**(2022)115101.
- [71] Karmarkar, K.R.: Proc. Indian Acad. Sci. A **27**(1948)56.
- [72] Maurya, S.K. and Maharaj, S.D.: Eur. Phys. J. C **77**(2017)13.
- [73] Bhar, P., Singh, K.N., Sarkar, N. and Rahaman, F.: Eur. Phys. J. C **77**(2017)596.
- [74] Naidu, N.F., Govender, M. and Maharaj, S.D.: Eur. Phys. J. C **78**(2018)7.
- [75] Singh, K.N., Bisht, R.K., Maurya, S.K. and Pant, N.: Chin. Phys. C **44**(2020)035101.
- [76] Mustafa, G., Shamir, M.F. and Ahmad, M.: Phys. Dark Universe **30**(2020)100652.
- [77] Mustafa, G., Shamir, M.F. and Tie-Cheng, X.: Phys. Rev. D **101**(2020)104013.
- [78] Maurya, S.K., Al Kindi, A.S., Al Hatmi, M.R. and Nag, R.: Results Phys. **29**(2021)104674.
- [79] Naz, T., Usman, A. and Shamir, M.F.: Ann. Phys. **429**(2021)168491.
- [80] Malik, A., Mofarreh, F., Zia, A. and Ali, A.: Chin. Phys. C **46**(2022)095104.
- [81] Bhar, P., Singh, K.N. and Manna, T.: Int. J. Mod. Phys. D **26**(2017)1750090.
- [82] Singh, K.N. Pant, N. and Govender, M.: Eur. Phys. J. C **77**(2017)11.
- [83] Rawls, M.L. et al.: Astrophys. J. **730**(2011)25.
- [84] Elebert, P. et al.: Mon. Not. R. Astron. Soc. **395**(2009)884.

- [85] Abubekerov, M.K. et al.: *Astron. Rep.* **52**(2008)379.
- [86] Ozel, F., Guver, T. and Psaltis, D.: *Astrophys. J.* **693**(2009)1775.
- [87] Deb, D. et al.: *Ann. Phys.* **387**(2017)239.
- [88] Shamir, M.F. and Zia, S.: *Eur. Phys. J. C* **77**(2017)448.
- [89] Buchdahl, A.H.: *Phys. Rev. D* **116**(1959)1027.
- [90] Ivanov, B.V.: *Phys. Rev. D* **65**(2002)104011.
- [91] Bejger, M. and Haensel, P.: *Astron. Astrophys.* **396**(2002)3.
- [92] Tolman, R.C.: *Phys. Rev.* **55**(1939)364; Oppenheimer, J.R. and Volkoff, G.M.: *Phys. Rev.* **55**(1939)374.
- [93] Herrera, L.: *Phys. Lett. A* **165**(1992)206.
- [94] Chandrasekhar, S.: *Astrophys. J.* **140**(1964)417.
- [95] Salako, I.G. et al.: *Universe* **6**(2020)167; *Int. J. Mod. Phys. D* **30**(2021)2140003.
- [96] Das, S. et al.: *Ann. Phys.* **433**(2021)168597.
- [97] Yousaf, Z. et al.: *Eur. Phys. J. C* **77**(2017)691.
- [98] Sharif, M. and Gul, M.Z.: *Fortschr. der. Phys.* **71**(2023)2200184.